Application Note 64-1

Fundamentals of RF and Microwave Power Measurements

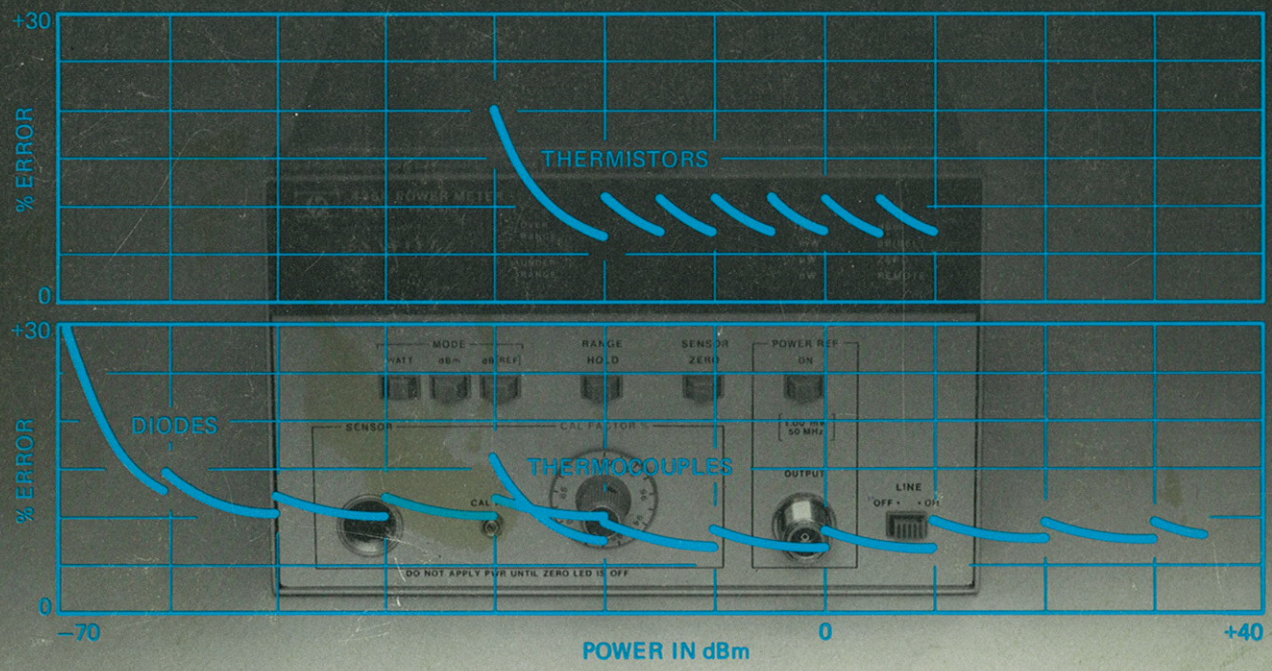

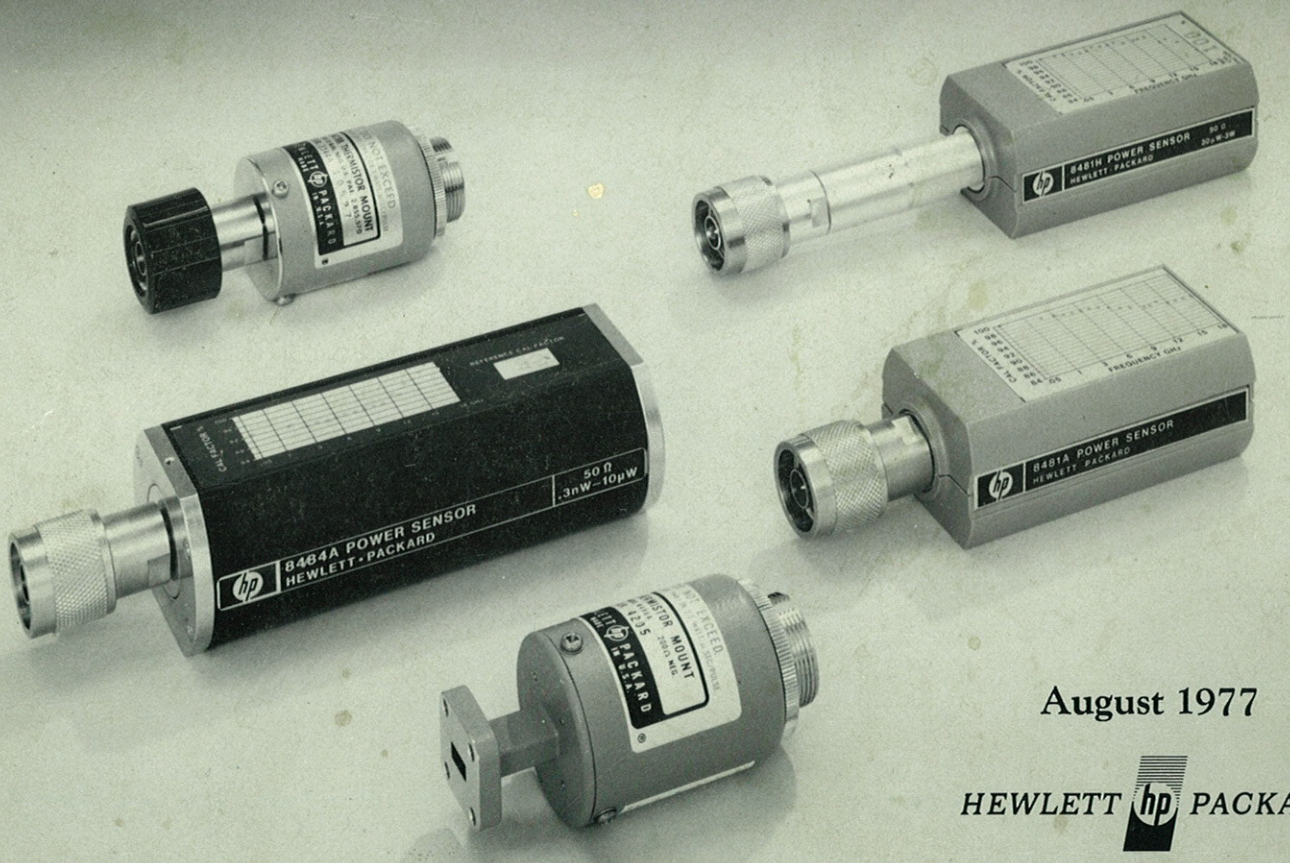

August 1977

HEWLETT hp PACKARD

Application Note 64-1

Fundamentals of RF and Microwave Power Measurements

August 1977
Revised June 1978

HEWLETT hp PACKARD

Contents

List of Symbols

a_g incident wave upon a generator
a_ℓ incident wave upon a load
b_g emerging wave from a generator
b_ℓ reflected wave from a load
b_s generated wave of a source
CW continuous wave
C, C_1, C_2 capacitors
C_b bypass capacitance
C_c coupling capacitance
C_o diode junction capacitance
e instantaneous voltage
e_p peak voltage
e_s source voltage
E_{rms} root mean-square of a voltage waveform
f_m maximum modulation frequency component
f_r repetition frequency
i instantaneous current
i instrumentation uncertainty
i_ℓ load current
i_p peak current
I_{rms} root mean-square of a current waveform
I_s diode saturation current
K Boltzmann's constant
K_b calibration factor
L inductance
L_w wire lead inductance
m magnification (gain)
m_i instrument magnification uncertainty
M_u mismatch uncertainty
n a number
NBS National Bureau of Standards (USA)
p product of voltage and current
P power
P_{av} available generator power
P_{avg} average power
P_p pulse power
P_d dissipated power
P_{fs} power at full scale
$P_{g\ell}$ net power transferred to load from generator
P_{gZo} power delivered to Z_o load from generator
P_i incident power
P_m meter indication of power
P_r reflected power
P_{ref} reference power
P_{rf} radio frequency power
P_{sub} substituted power, dc or low frequency equivalent of an rf power
q charge
rf radio frequency
rss root-sum-of-the-squares
R_c resistance of compensating thermistor
R_d resistance of detecting thermistor
R_o diode origin resistance
R, R_1, R_2, R_L resistor
R_b bulk resistance of silicon
R_s source resistance
R_T thermistor resistance
S_1 to S_6 Switches
t time as a variable
t translation (offset) error
T temperature in K
T time lapse
T_o period of a waveform
T_ℓ period of the lowest frequency
T_r period of the repetition frequency
v instantaneous voltage
v_ℓ voltage across a load
v_o output voltage
V_0, V_1, V_2, V_T Voltages
V_c Voltage driving the compensating bridge
V_h Peltier emf at a hot junction
V_{rf} voltage driving the rf thermistor bridge
V_{rfo} voltage driving the rf thermistor bridge when no rf power is applied
Z_o reference impedance
Z_g generator impedance
Z_ℓ load impedance
α q/nKT
Γ_g complex reflection coefficient looking back into a generator
Γ_ℓ complex reflection coefficient of a load
η_e effective efficiency
ρ_ℓ reflection coefficient magnitude of a load
ρ_g reflection coefficient magnitude of a generator
τ pulse width
ϕ phase angle between a sinusoidal waveform and a reference waveform
ϕ_g reflection coefficient angle of a generator
ϕ_ℓ reflection coefficient angle of a load

I. Introduction

This application note, AN 64-1, is the first of a series about rf and microwave power measurement. This first note reviews the instruments used for measuring power, discusses error mechanisms, and gives principles for calculating overall measurement accuracy. Other notes of the series discuss specific techniques and measurement set-ups, both for traditional power measurement applications and for more sophisticated applications using automatic measurement techniques and data processing.

This introductory chapter discusses units, defines such terms as average power and pulse power, and shows the path of traceability from a routine power measurement to the United States National Reference Standard. Chapters II, III, and IV go into detail about instrumentation for measuring power with the three most popular power sensing methods: thermistors, thermocouples, and diode detectors. Chapter V is about mismatch errors and Chapter VI discusses the remaining errors of power measurements as well as the calculation of overall uncertainty. Chapter VII compares the three popular methods for measuring average power. Peak and pulse power measurement equipment is discussed in Chapter VIII.

The Importance of Power

Operating power level is frequently the critical factor in the design and ultimately in the performance and purchase of almost all radio frequency and microwave equipment. A ten-watt transmitter, for example, costs more than a five-watt transmitter. Twice the power output means twice the geographical area is covered or 40 percent more range for a communication system.

Because power level is so important to the overall system, it is also very important in specifying the components that make up the system. Each component must receive the proper signal level from the previous component and pass the proper level to the succeeding component. If the power level becomes too low, the signal becomes obscured in noise. If the level gets too high, distortion results. It is also at the higher operating power levels where every dB increase in level is often costly in terms of complexity of design, expense of active devices, skill in manufacture, difficulty of testing, and decreased reliability. The increased cost per dB of level is especially true at microwave frequencies, where the maximum allowed power levels of solid state devices are close to minimum acceptable performance levels for systems.

The measurement of power is therefore critical at every level, from the overall system to the fundamental devices. Power is so important that it is frequently measured twice at each level, once by the manufacturer and again by the acceptor before beginning the next level. Many systems continuously monitor the power during ordinary operation. The large number and importance of power measurements dictates that the measurement equipment and technique be accurate, repeatable, traceable, and convenient. The goal of this application note series is to guide the reader in making those qualities routine.

Because many of the examples cited above used the term "signal level," the natural tendency might be to measure voltage instead of power. At low frequencies, below about 100 kHz, power is usually calculated from voltage measurements. As the frequency increases, however, power measurement becomes more popular and voltage or current are the calculated parameters.

At frequencies from about 30 MHz on up through the optical spectrum, the direct measurement of power is more accurate and easier. As the frequency approaches 1 GHz, power measurements become more and more important because voltage and current begin to lose usefulness. One reason for this is that voltage and current vary with position along a lossless transmission line but power is constant. Another example of decreased usefulness is in waveguide where voltage and current are difficult to define and imagine. For these reasons, at radio and microwave frequencies, power flow is more measurable, easier to understand, and more useful than voltage or current as a fundamental quantity.

Units and Definitions

The International System of Units (SI) has established the watt (W) as the unit of power; one watt is one joule per second. Electrical quantities do not even enter into the definition of power. As a matter of fact, other electrical units are derived from the watt. A volt, for example, is one watt per ampere. By the use of appropriate standard prefixes the watt becomes the kilowatt (1 kW = 10^3 W), milliwatt (1 mW = 10^{-3} W), microwatt (1 μW = 10^{-6} W), nanowatt (1 nW = 10^{-9} W), etc.

dB

In many cases, such as when measuring gain or attenuation, the ratio of two powers, or relative power, is frequently desired rather than absolute power. Relative power is the ratio of one power level, P, to some other level or reference level, P_{ref}. The ratio is dimensionless because the units of both the numerator and

denominator are watts. Relative power is usually expressed in decibels (dB). The dB is defined by

$$dB = 10 \log_{10} \left(\frac{P}{P_{ref}} \right). \quad (1\text{-}1)$$

The use of dB has two advantages. First, the range of numbers commonly used is more compact; for example +63 dB to −153 dB is more concise than 2×10^6 to 0.5×10^{-15}. The second advantage is apparent when it is necessary to find the gain of several cascaded devices. Multiplication is then replaced by the addition of the power gain in dB for each device.

dBm

Popular usage has added another convenient unit, the dBm. The formula for dBm is like (1-1) except the denominator, P_{ref}, is always one milliwatt:

$$dBm = 10 \log_{10} \left(\frac{P}{1\ mW} \right) \quad (1\text{-}2)$$

In this expression, P is the only variable, so dBm is used as a measure of absolute power. An oscillator, for example, may be said to have a power output of 13 dBm. By solving for P in (1-2), the power output can also be expressed as 20 mW. So dBm actually means "dB above one milliwatt," but a negative number of dBm is to be interpreted as "dB below one milliwatt." The advantages of dBm parallel those for dB – compact numbers and the frequent use of addition instead of multiplication when cascading.

Power

The term "average power" is very popular and is used in specifying almost all rf and microwave systems.

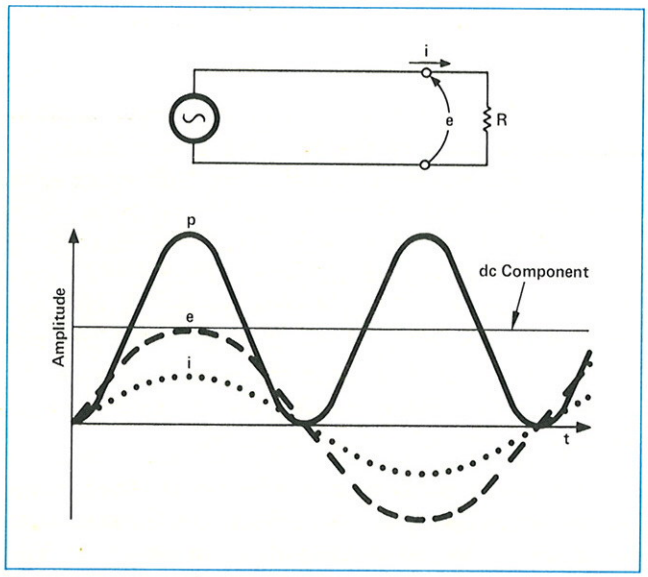

Figure 1-1. The product of voltage and current, p, varies during the sinusoidal cycle.

The terms "pulse power" and "peak envelope power" are more pertinent to radar and navigation systems. Before describing the instruments and methods for measuring these various terms, the definitions of each term should be discussed. Even before that, the meaning of the word "power" needs to be reviewed.

In elementary circuit theory, power is said to be the product of voltage and current. But for an ac cycle, this product varies during the cycle as shown by curve p in **Figure 1-1.** From that example a sinusoidal generator produces a sinusoidal current as expected, but the product of voltage and current has a dc term as well as a component at twice the generator frequency. The word "power," as used here, refers to that dc component of the product. All the methods of measuring power to be discussed use "power sensors" which, by averaging, select the dc component.

The fundamental definition of power is energy per unit time. This corresponds with the definition of a watt as energy transfer at the rate of one joule per second. The important question to resolve is: over what time is the energy transfer rate to be averaged when finding power? From **Figure 1-1** it is clear that if a narrow time slot is shifted around within the cycle, varying answers for energy transfer rate are found. But at radio and microwave frequencies such microscopic investigations of the voltage-current product are not common. Because of the techniques to be used in measurement, the word "power," throughout this application note, will mean the energy transfer rate averaged over many rf periods.

A more mathematical approach to power for a continuous wave (CW) is to find the average height under the curve of p in **Figure 1-1.** Averaging is done by finding the area under the curve, that is by integrating, and then dividing by the length of time over which that area is taken. The length of time should be an exact number of ac periods. The power of a CW signal at frequency $(1/T_o)$ is

$$P = \frac{1}{nT_0} \int_0^{nT_0} e_p \sin\left(\frac{2\pi}{T_0} t \right) \cdot i_p \sin\left(\frac{2\pi}{T_0} t + \phi \right) dt \quad (1\text{-}3)$$

where T_o is the ac period, e_p and i_p represent peak values of e and i, ϕ is the phase angle between e and i, and n is the number of ac periods. This yields (for n = 1, 2, 3 . . .)

$$P = \frac{e_p i_p}{2} \cos \phi \quad (1\text{-}4)$$

If the integration time is at least many ac periods long, then whether n is a precise integer or not makes a vanishingly small difference. This result for large n is the basis of power measurement.

For sinusoidal signals, circuit theory shows the relationship between peak and rms values as

$$e_p = \sqrt{2}\, E_{rms} \text{ and } i_p = \sqrt{2}\, I_{rms}$$

Using these in (1-4) yields the familiar expression for power

$$P = E_{rms} \cdot I_{rms} \cos \phi \qquad (1\text{-}5)$$

For this application note, power is defined as the energy transfer per unit time averaged over many periods of the highest frequency (rf or microwave) involved.

Average Power

"Average power," like the other power terms to be defined, places further restrictions on the averaging time than just "many periods of the highest frequency." Average power means the energy transfer rate is to be averaged over many periods of the lowest frequency involved. For a CW signal, the lowest frequency and highest frequency are the same so average power and power are the same. For an amplitude modulated wave, the power must be averaged over many modulation cycles. For a pulse modulated signal, power must be averaged over many repetitions of the pulse.

In a more mathematical sense, average power can be written as

$$P_{avg} = \frac{1}{nT_\ell} \int_0^{nT_\ell} e(t) \cdot i(t)dt \qquad (1\text{-}6)$$

where T_ℓ is the period of the lowest frequency component of e(t) and i(t).

The averaging time for average power measurements is typically from several hundredths of a second to several seconds and therefore averages most common forms of amplitude modulation.

Pulse Power

For pulse power the energy transfer rate is averaged over the pulse width τ. Pulse width τ is considered to be the time between the 50 percent amplitude points.

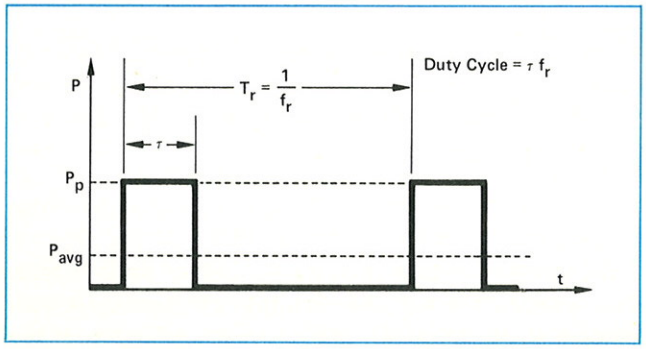

Figure 1-2. Pulse power P_p is averaged over the pulse width.

Mathematically, pulse power is given by

$$P_p = \frac{1}{\tau} \int_0^{\tau} e(t) \cdot i(t)dt \qquad (1\text{-}7)$$

By its very definition, pulse power averages out any aberrations in the pulse such as overshoot or ringing. For this reason it is called **pulse power** and not peak power or peak pulse power as is done in many radar references. Peak power and peak pulse power are totally avoided here for that reason.

The definition of pulse power has been extended since the early days of microwave to be

$$P_p = \frac{P_{avg}}{\text{Duty Cycle}} \qquad (1\text{-}8)$$

where duty cycle is the pulse width times the repetition frequency. This extended definition, which can be derived from (1-6) and (1-7) for rectangular pulses, allows calculation of pulse power from an average power measurement and the duty cycle.

Peak Envelope Power

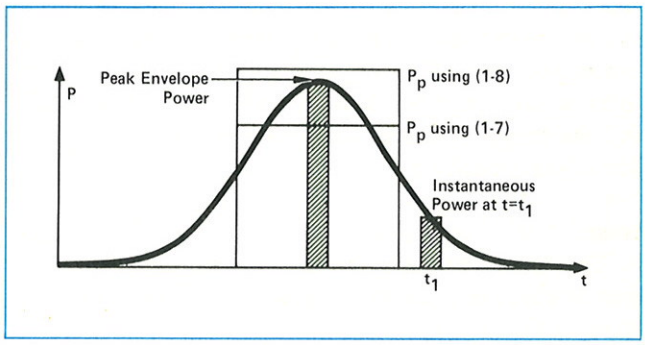

Figure 1-3. A Gaussian pulse and the different kinds of power.

For certain more sophisticated microwave applications, and because of the need for greater accuracy, pulse power is not totally satisfactory. Difficulties arise when the pulse is intentionally non-rectangular or when aberrations do not allow an accurate determination of pulse width τ. **Figure 1-3** shows the example of a Gaussian pulse shape, used in certain navigation systems, where pulse power, by either (1-7) or (1-8), does not give a true picture of power in the pulse. Peak envelope power is a term for describing the maximum power. Envelope power will first be discussed.

Envelope power is measured by making the averaging time much less than $1/f_m$, where f_m is the maximum frequency component of the modulation waveform. The averaging time is therefore limited on both ends: (1) it must be small compared to the period of the highest

modulation frequency, and (2) it must be large enough to be many rf cycles long.

By continuously displaying the envelope power on an oscilloscope, the oscilloscope trace will show the profile of the pulse shape. Peak envelope power is the maximum value of the envelope power (see **Figure 1-3**). For perfectly rectangular pulses, peak envelope power is equal to pulse power as defined above.

Average power, pulse power, and peak envelope power all yield the same answer for a CW signal. Of all power measurements, average power is the most frequently measured because of convenient measurement equipment with highly accurate and traceable specifications. Pulse power and peak envelope power can often be calculated from average power measurement. Average power measurements therefore occupy the greatest portion of this application note series.

Methods of Sensing Power

There are three popular methods of sensing and measuring average power at rf and microwave frequencies. Each of the methods uses a different kind of device to convert the rf power to a measureable dc or low frequency signal. The devices are the thermistor, the thermocouple, and the diode detector. Each of the next three chapters discusses in detail one of the devices and its associated instrumentation. Each method has some advantages and disadvantages over the others. After the individual measurement methods are studied, the overall measurement errors are discussed. Then the results of the three methods are summarized and compared in Chapter VII.

The general measurement technique for average power is to attach a properly calibrated sensor to the transmission line port at which the power is to be measured. The output from the sensor is connected to an appropriate power meter. The rf power to the sensor is turned off and the power meter is adjusted to read zero power. This operation is often referred to as zero-setting or zeroing. Power is then turned on, and the sensor, reacting to the new input level, sends a signal to the power meter, and the new meter reading is observed.

In the ideal case, the power sensor absorbs all the power incident upon the sensor. There are two categories of non-ideal behavior that are discussed in detail in Chapters V and VI, but need to be introduced here.

First, there is a likely impedance mismatch between the characteristic impedance of the rf transmission line and the rf input impedance of the sensor. Another way of stating this is that some of the power that is incident on the sensor is reflected back toward the generator rather than dissipated in the sensor. The relationship between incident power P_i, reflected power P_r, and dissipated power P_d, is

$$P_i = P_r + P_d \qquad (1\text{-}9)$$

The relationship between P_i and P_r for a particular sensor is given by the sensor reflection-coefficient magnitude ρ_e

$$P_r = \rho_e{}^2 \, P_i \qquad (1\text{-}10)$$

Reflection-coefficient magnitude is a very important specification for a power sensor because it contributes to the most prevalent source of error, mismatch uncertainty, which is discussed in Chapter V. An ideal power sensor has a reflection coefficient of zero; ρ_e of 0.05 or 5 percent is adequate for most situations whereas 40 percent would not be adequate for most situations.

The second cause of non-ideal behavior is that rf power might be dissipated in places other than in the power sensing element. Such losses are not metered. This defect is measured by the effective efficiency η_e. An effective efficiency of 1 (100%) means that all the dissipated power is absorbed by the sensing element and metered—no power is dissipated in conductors or other components of the sensor.

The most frequently used specification of a power sensor is called the calibration factor K_b. K_b is a combination of reflection coefficient and effective efficiency according to

$$K_b = \eta_e(1 - \rho_e{}^2) \qquad (1\text{-}11)$$

If a sensor has a K_b of 0.91 (91%) the power meter would normally indicate a power level that is 9 percent lower than the incident power P_i. Recent power meters, however, usually have the ability to correct the lower reading by setting a Calibration Factor dial on the power meter to correspond with the calibration factor of the sensor. Calibration factor correction is not capable of correcting for the total effect of reflection coefficient. There is still a mismatch uncertainty that is discussed in Chapter V.

Traceability

Since power measurement is so important for commercial reasons and for assuring that components can be interfaced to form a system, it is important that power measurements can be duplicated at different times and at different places. This requires well-behaved equipment, good measurement technique, and

common agreement as to what is the standard watt. The agreement, in the United States, is established by the National Bureau of Standards (NBS) at Boulder, Colorado, which maintains a National Reference Standard in the form of a microcalorimeter. When a power sensor can be referenced back to that National Reference Standard, the measurement is said to be traceable to NBS.

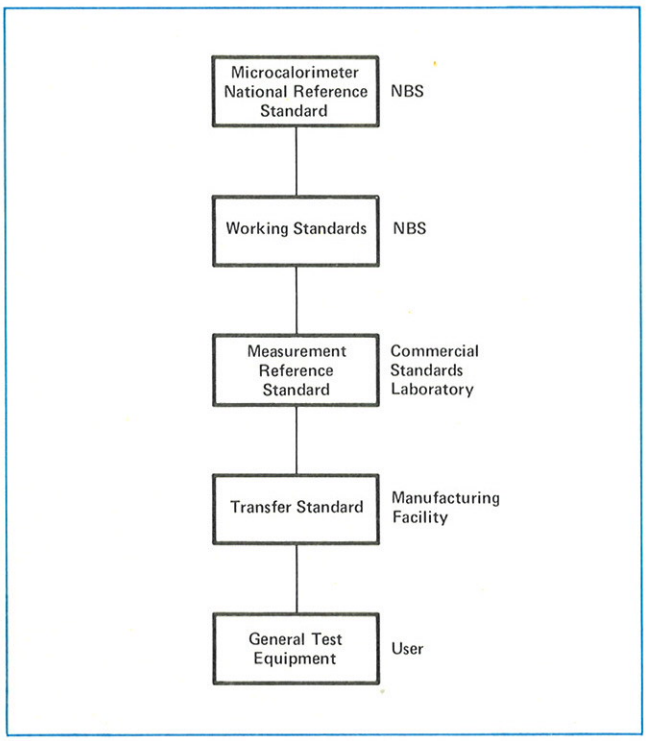

Figure 1-4. The traceability path of test equipment from the United States National Reference Standard.

The usual path of traceability for an ordinary power sensor is shown in **Figure 1-4.** At each echelon at least one power standard is maintained. That power sensor is periodically sent to the next higher echelon for recalibration, then returned to its original position. Recalibration intervals are established by observing the stability of a device between successive recalibrations. A device might be recalibrated every few months. Then, when the calibration is seen not to change, the interval can be extended to a year or so.

Each echelon along the traceability path adds some uncertainty. Extreme care is exercised at the top level because any error at that level must be included in the total uncertainty at every lower level. As a result of this extreme care, the cost of calibration tends to be greatest at the top level and least at the bottom. The measurement technique for calibrating a power sensor against one at a higher echelon is discussed in another note of this series.

Many of the power sensors used in test equipment are physically capable of serving as a standard at a higher level. All that is needed is proper calibration. It is therefore possible, though expensive, to have a sensor that is used as general test equipment, calibrated by NBS against the NBS Working Standards.

Because the National Reference Standard is a microcalorimeter, calorimetry plays a fundamental role in power measurement. With the exception of standards laboratories such as NBS, calorimetric techniques are seldom used anymore. The technique is used for fundamental measurement because electrical power can be related directly to the rate of flow of heat, that is, back to the definition of the watt as one joule per second.

The main disadvantage of calorimetric techniques is that a significant amount of equipment is usually required, sometimes including liquids and pumps to carry heat. Portable measurements are therefore difficult. The Hewlett-Packard 434A Calorimetric Power Meter was portable and relied on oil flow to measure power over a range of 10 mW to 10 W (10 to 40 dBm). The modern thermocouple sensor has encroached on the 434A power range, with greater accuracy, to such an extent that the 434A is no longer produced.

II. Thermistor Mounts and Instrumentation

Bolometers are power sensors that operate by changing resistance due to a change in temperature. The change in temperature results from converting rf energy into heat within the bolometric element. There are two principle types of bolometers, barretters and thermistors. A barretter is a thin piece of wire that has a positive temperature coefficient of resistance. Thermistors are semiconductors with a negative temperature coefficient.

To have a measureable change in resistance for a small amount of dissipated rf power, a barretter is constructed of a very thin and short piece of wire. The maximum power that can be measured is limited by the burnout level of the barretter. The automatic Wheatstone bridges, used to monitor rf power, maintain bridge balance by means of biasing the barretter so the total power dissipated is just above the largest rf power level that can be measured. The result of the small size and high operating power level is that the barretter operates very close to burnout. The barretter is so easily destroyed by accidental or transient overloads that it is seldom used anymore. In the early days of microwave development, however, barretters were popular because they were readily available in the form of 10 mA fuses originally developed for instrument protection. The reason for mentioning barretters is mainly historical; the older, standard references discuss them and most power meters built before 1961 worked with barretters and thermistors.

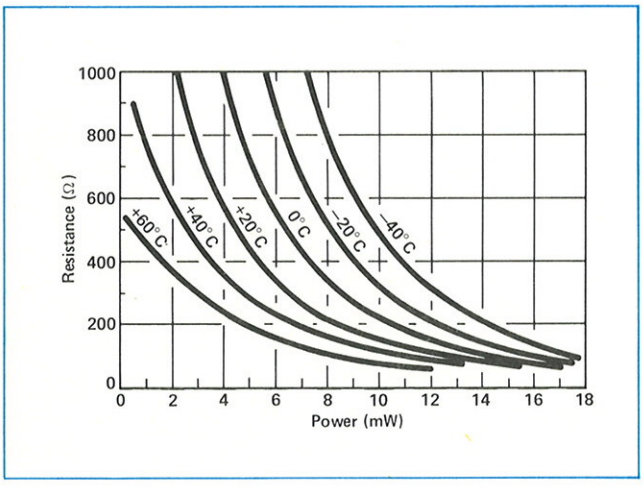

Figure 2-1. Characteristic curves of a typical thermistor bead used for sensing power.

The thermistor used for rf power measurement is a small bead of metallic oxides typically 0.4 mm diameter with 0.03 mm wire leads. From a graph of thermistor characteristics **(Figure 2-1)** resistance vs. power is seen to be highly non-linear. The curves also vary considerably from one thermistor to the next. To depend on the precise, quantitative shape of such curves would result in difficult and complicated power measurements. Instead, the technique is to always maintain the thermistor at a constant resistance R by means of dc or low frequency bias. As rf power is dissipated in the thermistor, tending to lower R, the bias power is decreased by just the proper amount to keep R the same value. The decrease in bias power should be identical to the increase in rf power. That decrease in bias power is then displayed on a meter to indicate rf power. Bridges are used to monitor the resistance.

Thermistor Mounts

Thermistor elements are mounted in either coaxial or waveguide structures so they are compatible with common transmission line systems used at microwave and rf frequencies. The thermistor and its mount must be designed to satisfy several important requirements so that the thermistor element will absorb as much of the power incident on the mount as possible. First, the mount must present a good impedance match to the transmission line over the specified frequency range. The mount must also have low resistive and dielectric losses within the mounting structure because only power that is dissipated in the thermistor can be registered on the meter. In addition, mechanical design must provide isolation from thermal and physical shock and must keep leakage small so that microwave power does not escape from the mount in a shunt path around the thermistor. Shielding is also important to prevent extraneous power from entering the mount.

More recent thermistor mounts have a second thermistor or set of compensating thermistors to correct for ambient temperature variations. These compensating thermistors are matched in their temperature-resistance characteristics to the detecting thermistors. The thermistor mount is designed to maintain electrical isolation between the detecting and compensating thermistors while keeping the thermistors in thermal contact.

Coaxial Thermistor Mounts

The HP 478A Thermistor Mount contains four matched thermistors, electrically connected as in **Figure 2-2.** The two detecting thermistors, R_d, are connected in series as far as the low frequency bridge circuits are concerned. For rf frequencies, the two R_d thermistors are connected in parallel, being driven

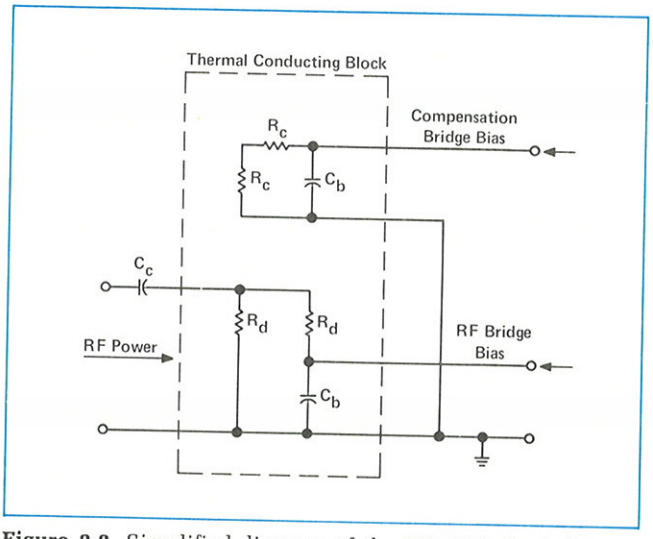

Figure 2-2. Simplified diagram of the HP 478A dual-element temperature compensating, coaxial thermistor mount.

through coupling capacitor C_c. The lower node of the left R_d thermistor is directly connected to ground and the lower node of the right R_d thermistor is at rf ground through bypass capacitor C_b. Each thermistor is biased to a resistance of 100 ohms. A total resistance of 200 ohms is therefore in the thermistor arm of the bridge. But the rf input sees a 50 ohm terminating resistance for the transmission line. The principle advantage of this connection scheme is that both leads to the bridge are at rf ground; there is no need for an rf choke in the upper lead. Such a choke would likely limit the frequency range of the thermistor mount.

Compensating thermistors R_c, which are to monitor changes in ambient temperature but not changes in rf power, are also connected in series. These thermistors are biased to a total of 200 ohms by a different bridge of the power meter called the compensating bridge. The compensating thermistors are completely enclosed in a cavity for electrical isolation from the rf signal. They are mounted on the same thermal conducting block as the detecting thermistors. The thermal mass of the block is large enough to prevent sudden temperature gradients across the thermistors.

There is a particular error, called Dual Element Error, that is limited to coaxial thermistor mounts where the two thermistors are in parallel for the rf energy, but in series for dc. If the two thermistors are not quite identical in resistance, then more high frequency current will flow in the one of least resistance, but more dc power will be dissipated in the one of greater resistance. The lack of equivalence in the dissipated dc and rf power is a source of error that is proportional to power level. For Hewlett-Packard thermistor mounts this error is less than 0.1 percent at the high power end of their measurement range and is therefore considered as insignificant in the error analysis of Chapter VI.

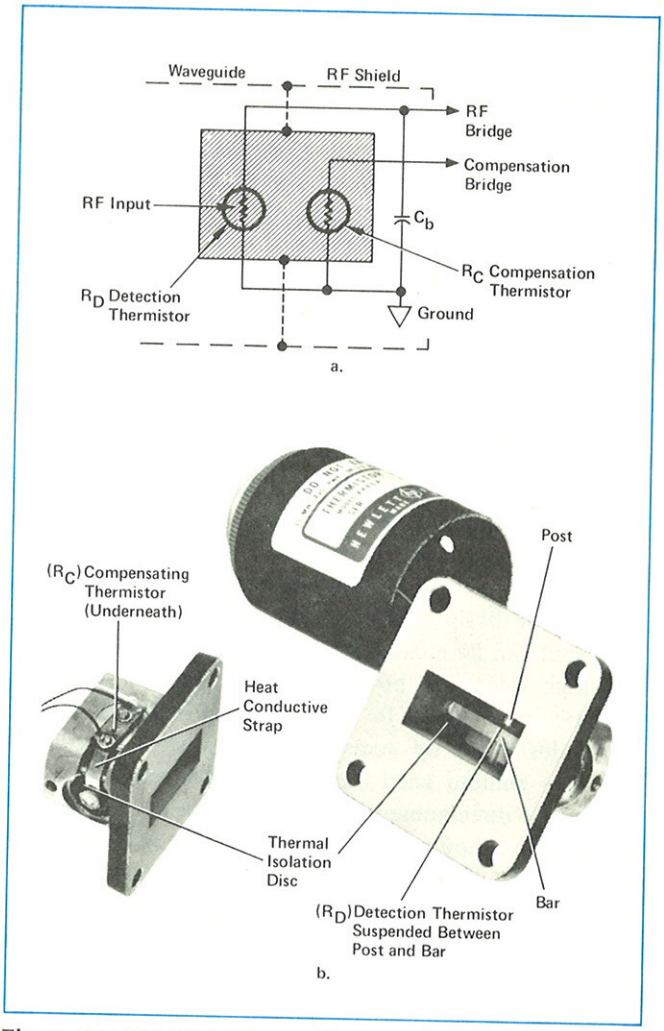

Figure 2-3. HP 486A Waveguide Thermistor Mount: (a) circuit, (b) construction.

The HP 478A is designed for coaxial power measurements over 10 MHz to 10 GHz with a maximum reflection coefficient of 0.2 over most of its range. The HP 8478A coaxial Thermistor Mount uses the same principles as the 478A. The construction, however, is upgraded in order to gain operation to 18 GHz with a maximum reflection coefficient of 0.23 over most of that range.

Waveguide Thermistor Mounts

The HP 486A Series of waveguide thermistor mounts covers frequencies to 40 GHz. The waveguide mounts for use up to 18 GHz utilize a post-and-bar mounting arrangement for the detecting thermistor. Detecting thermistor R_d is a single bead, 100 ohm thermistor

mounted with its axis parallel to the **E** field and centered in the waveguide. **Figure 2-3a** shows the electrical configuration of R_d and the compensating thermistor R_c. **Figure 2-3b** shows the post and bar which are thermally isolated from the waveguide structure by a circular section of glass epoxy. Electrical continuity across the epoxy is obtained by a thin gold plating on the epoxy surface inside the guide. This thin plating minimizes heat flow from the waveguide to the bar and thermistor element. Thus the thermistor is isolated from ambient temperature changes but is in good electrical contact with the waveguide. The detection thermistor is further isolated from ambient changes by a block of polystyrene foam inserted into the waveguide opening. The foam prevents air currents from changing the temperature of R_d and protects the tiny thermistor bead from foreign objects which could enter the waveguide input. The foam has little net effect on the reflection coefficient and does not change the effective efficiency. Compensating thermistor R_c is also a single bead which is thermally strapped to the bar. The thermistors and the bypass capacitor C_b are shielded by a metal case which helps prevent convective thermal changes from reaching the thermistors.

The 486A Series mounts covering the K and R waveguide band (18 to 26.5 GHz and 26.5 to 40 GHz) utilize smaller thermistors which are biased to an operating resistance of 200 ohms rather than the 100 ohms used in lower frequency waveguide units but are schematically the same as that shown in **Figure 2-3a.**

Because some thermistor mounts are designed for 200 ohm operation and others for 100 ohm operation, power meters have a switch for selecting the proper bridge circuitry for the thermistor mount being used.

Bridges

Over the years, Wheatstone bridges for monitoring and regulating power sensing thermistors have gone through quite an evolution. The first bridges were unbalanced by the presence of rf changing the element resistance. The degree of unbalance was then monitored on a meter and related to rf power by calibration charts. The technique had many drawbacks. The most serious was that the element resistance varied with rf power level which meant that the reflection coefficient also varied with power level. The dynamic range was therefore limited to roughly a 2 mW range in the knee of the thermistor curve **(Figure 2-1).**

It wasn't long before a balanced bridge approach was used. As the rf power would increase, unbalancing the bridge, the operator would bring the bridge back into balance by decreasing the dc or low frequency bias through the bolometer. As stated previously, the decrease in bias power to rebalance the bridge is the same as the increase in rf power. Between monitoring bridge balance and measuring the dc and audio frequency bias, several meter readings were needed. The procedure was lengthy and required calculation, but the bolometer element was maintained at the same point of its resistance-power characteristic **(Figure 2-1).** This not only gave a constant reflection coefficient with power level, but also eliminated the need for using resistance-power calibration curves. The substituted, low-frequency power could be measured quite accurately. This technique was used to achieve a dynamic range of about 20 dB in the HP Model K04-999D bridge.

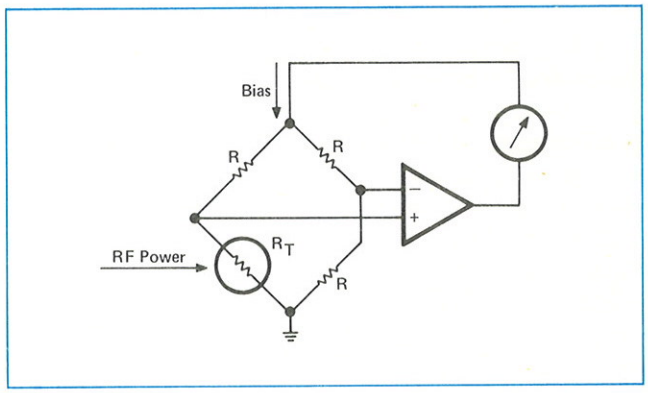

Figure 2-4. Simplified diagram of a self-balancing Wheatstone bridge.

The next step in the evolution was the self-balancing bridge, shown in simplified form in **Figure 2-4.** The bridge operated with both dc and audio bias. As the rf input would increase and change thermistor resistance, bridge unbalance would be sensed by the amplifier. The amplifier, being in a feedback loop, would automatically decrease the audio bias just enough to bring the bridge back into balance. Since the decrease in audio power is the same as the increase in rf power, the decrease in audio power was metered to indicate the rf power input. The HP 430C Microwave Power Meter was the most popular instrument that used this technique. The 430C was fast, convenient, and sophisticated for its day, but simple in comparison to modern instruments. Full scale ranges covered 20 dB, so the effective dynamic range was at least 25 dB.

The main drawback of the simple, self-balancing bridge was that the thermistor resistance would also change with changes in ambient temperature. Touching a thermistor mount with the hand, for example, would cause a resistance change, a consequent change in bridge bias power, and would show up as an erroneous change in the rf power level. The next level of sophisti-

cation is to use the temperature compensated thermistor mount explained above. This mount contains a second thermistor for sensing ambient temperature changes.

The Temperature Compensating Power Meter

The first generation of power meters for temperature compensated thermistor mounts culminated in the HP 431C Power Meter. This generation included the first completely solid state instruments. In the 431C the detecting bridge was automatically kept in balance by audio bias and feedback at 10 kHz in the manner described above for the 430C. That same 10 kHz audio bias was also fed through a transformer to the compensating thermistor bridge. The compensating bridge, with the 10 kHz bias from the rf bridge, was kept in balance by feedback amplifiers using dc bias. The dc power changes were metered. For a more detailed explanation of operation, consult the reference by Pramann.

Although the 431C was a great improvement over the 430C in dynamic range (10 dB more sensitive), in the instrumentation accuracy (1% vs. 5%), and in convenience (zero-setting the meter on the most sensitive range would carry over to the other ranges), significant improvements were still needed. For one thing, FET's were soon available so the possibility of automatically and electronically setting the zero was possible. Secondly, in coaxial mounts, the 10 kHz signal would not be completely blocked by the coupling capacitor C_c **(Figure 2-2).** In some circumstances this 10 kHz signal would cause problems in the rf energy source. This was especially true with solid state sources where a small amount of the 10 kHz bias could be coupled to the source and affect the operating point of the source devices. In a few other circumstances, the rf source would present different 10 kHz impedances to the thermistor mount during the power-off, zero-setting operation and during the power-on, rf measurement. This would change the effective zero-setting and cause an error.

Still another effect was thermoelectric. Small, thermocouple-type voltages were within the bridge circuits which ideally should have cancelled in the overall measurement. In practice, however, cancellation was not complete. In certain kinds of measurements this could cause an error of 0.3 μW. In the more modern bridge, soon to be discussed, the thermoelectric voltages are so small, compared to the metered voltages, as to be insignificant.

Power Meters with Automatic DC Bridges

The more recent generation of thermistor bridges takes advantage of newer solid-state technology espe-

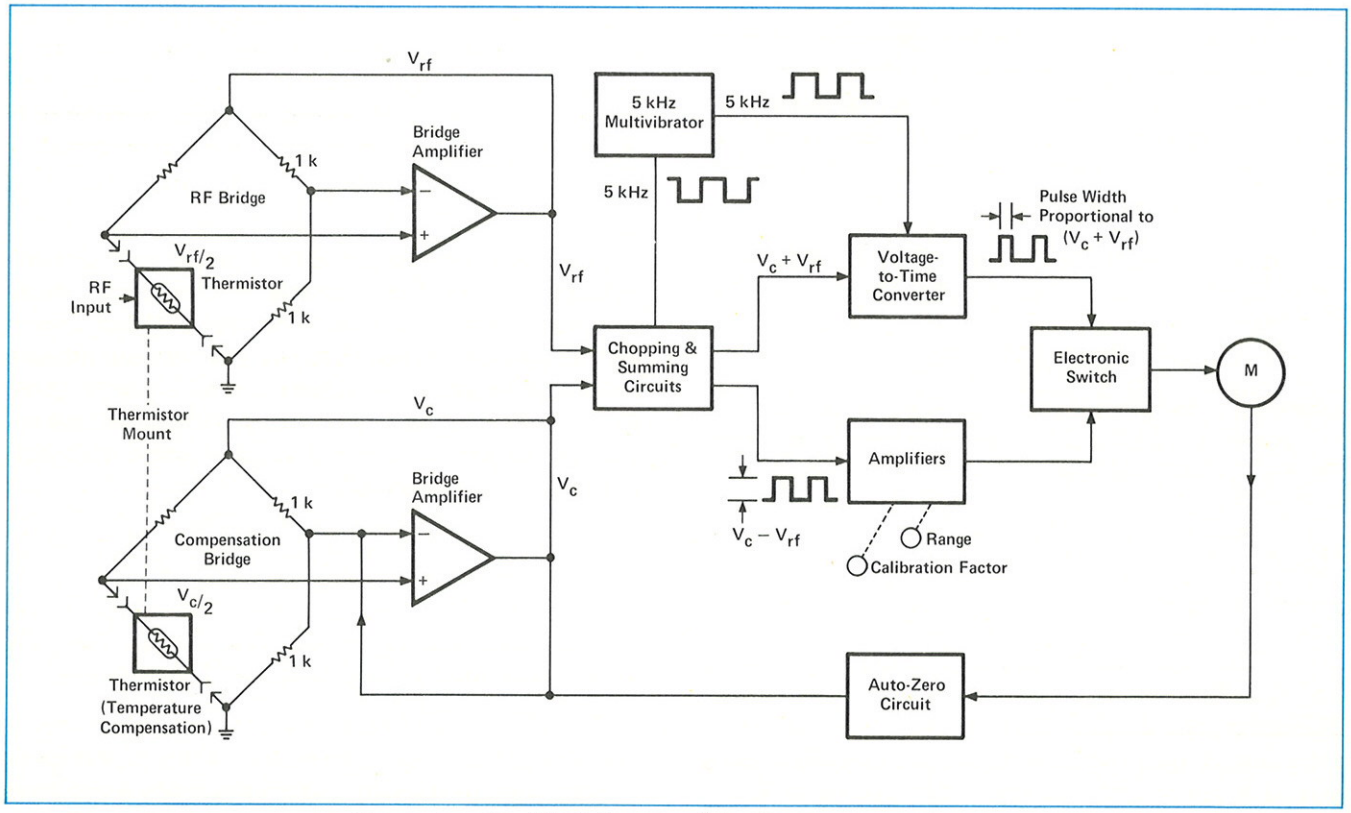

Figure 2-5. Simplified diagram of the HP 432A Power Meter.

cially the ease of designing dc amplifiers. This kind of power meter, exemplified by the HP 432A Power Meter, uses dc and not audio frequency power to maintain balance in both bridges. This eliminates the problems pertaining to the 10 kHz signals applied to the thermistors. The HP 432A has the further convenience of an automatic zero set, eliminating the need for the operator to precisely set a potentiometer. The 432A also carries an instrumentation accuracy of ±1 percent and uses the same temperature compensated thermistor mounts designed for the 431C Power Meters. Full scale ranges of measurement are from −20 dBm (10 μW) to +10 dBm (10 mW). The typical time constant of the recorder output of the 432A is 35 ms.

The principal parts of the 432A **(Figure 2-5)** are two self-balancing bridges, the meter logic section, and the auto-zero circuit. The rf bridge, which contains the detecting thermistor, is kept in balance by automatically varying the dc voltage V_{rf}, which drives that bridge. The compensating bridge, which contains the compensating thermistor, is kept in balance by automatically varying the dc voltage V_c, which drives that bridge. If one of the bridges is unbalanced due to incorrect thermistor resistance, an error voltage is applied to the top of the bridge and changes the power dissipation in the thermistor. The change of power dissipation causes the resistance of the thermistor to change in the direction required to balance the bridge.

The power meter is initially zero-set with no applied rf power by making V_c equal to V_{rfo} (V_{rfo} means V_{rf} with zero rf power). After zero-setting, if ambient temperature variations change thermistor resistance, the bridge circuits each respond by applying the same new voltage to maintain balance.

If rf power is applied to the detecting thermistor, V_{rf} decreases so that

$$P_{rf} = \frac{V_{rfo}^2}{4R} - \frac{V_{rf}^2}{4R} \qquad (2\text{-}1)$$

where P_{rf} is the rf power applied and R is the value of the thermistor resistance at balance. But from zero-setting, $V_{rfo} = V_c$ so that

$$P_{rf} = \frac{1}{4R}(V_c^2 - V_{rf}^2) \qquad (2\text{-}2)$$

which can be written

$$P_{rf} = \frac{1}{4R}(V_c - V_{rf})(V_c + V_{rf}) \qquad (2\text{-}3)$$

The meter logic circuitry is designed to meter the product shown in (2-3). Ambient temperature changes cause V_c and V_{rf} to change so there is zero change to $V_c^2 - V_{rf}^2$ and therefore no change to the indicated P_{rf}.

The $V_c - V_{rf}$ signal is obtained by taking the dc voltage outputs from the bridges and applying them to a chopper circuit. This chopper circuit is driven by a 5 kHz multivibrator. The output of the chopper is a square wave signal whose peak-to-peak amplitude is proportional to $(V_c - V_{rf})$. The output of the chopper is coupled to an amplifier whose gain depends upon the setting of the RANGE switch and the CALIBRATION FACTOR switch. The output of the amplifier is a current proportional to $(V_c - V_{rf})$. This current is fed through the electronic switch whenever the switch is closed.

The $(V_c + V_{rf})$ signal is obtained by taking the two dc voltages from the bridge assembly through a summing circuit and feeding this voltage to a voltage-to-time converter. The voltage-to-time converter is also driven by the 5 kHz multivibrator. The output of the converter is a pulse whose width is proportional to the sum $(V_c + V_{rf})$. This signal controls the timing of the electronic switch.

If the current coming through the switch has a pulse width proportional to $(V_c + V_{rf})$ and a height proportional to $(V_c - V_{rf})$, then the area under the pulse of current is proportional to $(V_c - V_{rf})(V_c + V_{rf})$. Those current pulses are integrated in a capacitor and a meter reads the capacitor voltage.

The principal sources of instrumentation uncertainty of the 432A lie in the metering logic circuits. But V_{rf} and V_c are both available at the rear panel of the 432A. With precision digital voltmeters and proper procedure, those outputs allow the instrumentation uncertainty to be reduced to ±0.2 percent for some measurements. The procedure is described in the operating manual for the HP 432A.

The thermistor power meter is also available with digital output for data processing and automatic operation. The HP 432B Power Meter has a digital display and BCD output. Range changing and zero setting must be performed with the manual controls. The HP 432C Power Meter not only has digital readout, but also is completely programmable including range selection, auto ranging, and auto zero.

Conclusions

There are some advantages to thermistor power measurements that have not been obvious from the above discussion or from data sheet specifications.

The electronic circuits in thermistor power meters operate at levels that are very convenient. Signal levels are high enough so as not to require special shielding in the usual industrial environments.

The fundamental premise in using a thermistor for power measurements is that the rf power absorbed by the thermistor has the same heating effect on the thermistor as the dc power. The feedback mechanism of the self-balancing bridge will always try to adjust the resistance back to the design value by varying the bias power. Even if the thermistor characteristics change due to aging, minor misuse, etc. the feedback mechanism will still bring the thermistor resistance back to the design value. The measurement is said to be "closed loop," because the feedback loop corrects for minor device irregularities. The technique is known as dc substitution because dc power is decreased as rf power is increased.

III. Thermocouple Sensors and Instrumentation

The use of thermocouples to sense rf and microwave power has progressed in recent years to give broader range and more accurate measurements than the thermistor techniques of the previous chapter. This evolution is the result of combining thin-film and semiconductor technologies to give a thoroughly understood, accurate, rugged, and reproducible power sensor. This chapter describes the principles of thermocouples, the construction and design of modern thermocouple sensors, and the instrumentation used to measure the rather small signal levels.

Principles of Thermocouples

Thermocouples generate a voltage due to temperature differences along the thermocouple. As a simple example of the kind of physics involved, imagine a long metal rod that is heated at the left end as in **Figure 3-1.** Because of the increased thermal agitation at the left end, many additional electrons become free from their parent atoms. The increased density of electrons at the left causes diffusion toward the right. There is also a force attempting to diffuse the positive ions to the right but the ions are locked into the metallic structure and cannot migrate. So far, this explanation has not depended on Coulomb forces. The migration of electrons toward the right is by diffusion, the same physical phenomenon that tends to equalize the partial pressure of a gas throughout a room, for example.

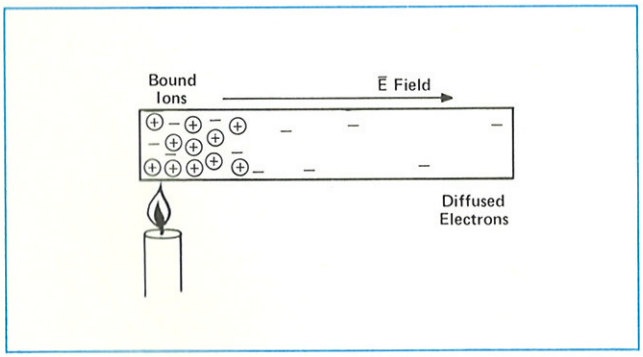

Figure 3-1. Heat at one end of a metal rod gives rise to an electric field.

Each electron that migrates to the right leaves behind a positive ion. That ion tends to attract the electron back to the left with a force given by Coulomb's law. The rod reaches equilibrium when the rightward force of diffusion is exactly balanced by the leftward force of Coulomb's law. The leftward force can be represented by an electric field pointing toward the right. The electric field, summed up along the length of the rod, gives rise to a voltage source, called the Thomson emf. This explanation is greatly simplified but it does indicate the principle.

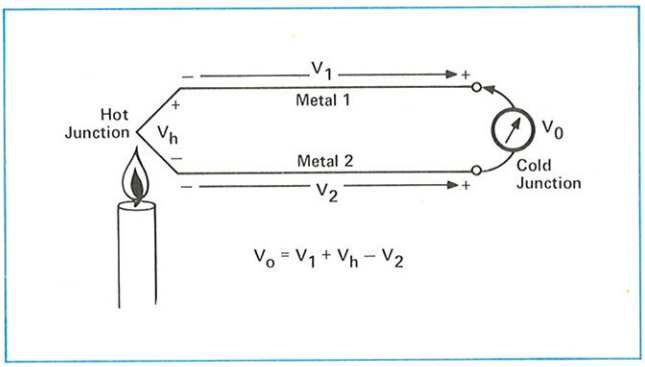

Figure 3-2. Total thermocouple output is the resultant of several thermoelectric voltages generated along the circuit.

The same principles apply at a junction of dissimilar metals, where different free electron densities in the two metals give rise to diffusion and an emf. The name of this phenomenon is the Peltier effect.

A thermocouple is usually a loop or circuit of two different materials as shown in **Figure 3-2.** One junction of the materials is exposed to the heat, the other is not. The complete loop is broken once to insert a sensitive voltmeter for measuring the net emf. The thermocouple loop uses both the Thomson emf and the Peltier emf to produce the net thermoelectric voltage. The total effect is also known as the Seebeck emf.

Sometimes, many pairs of junctions or thermocouples are connected in series so that the first junction of each pair is exposed to heat and the second is not. In this way the net voltage produced by one thermocouple adds to that of the next, and the next, etc., yielding a larger thermoelectric output. Such a series connection of thermocouples is called a thermopile.

The traditional thermocouple for sensing rf power is frequently constructed of bismuth and antimony. In order for one junction to get hot in the presence of rf energy, the energy is dissipated in a resistor constructed of the metals making up the junction. The metallic resistor must be small in length and cross section in order to have: a high enough resistance to be a suitable termination for a transmission line, a measureable change in temperature for the minimum power to be measured, and a uniform frequency response. Thin-film techniques are normally used to build metallic thermocouples. These small metallic thermocouples tend to have parasitic reactances and low burnout levels. Large thermopiles tend to be plagued by reactive effects at microwave frequencies because device dimensions become significant with respect to a wavelength.

The Modern Thermocouple

The modern thermocouple, exemplified by the HP 8481A Power Sensor, has taken advantage of both semiconductor and thin-film technologies. A thin-film resistor, constructed of tantalum nitride and deposited on the surface of a silicon chip, converts the microwave energy to heat. The tantalum-nitride resistive material forms a low-reflection termination for the rf transmission line to frequencies above 18 GHz. Yet the resistor is not at all fragile in contrast to similar terminations constructed of a highly conductive material like most metals. It is largely because of this thin-film resistor that the thermocouple sensor has the lowest reflection coefficient of all the sensing methods.

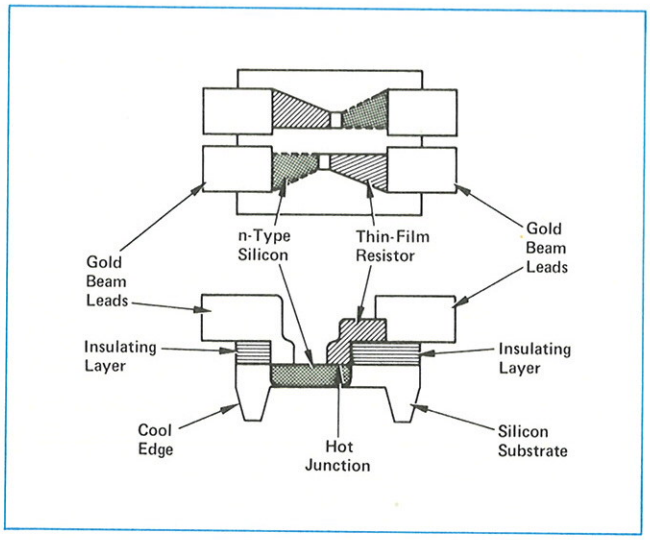

Figure 3-3. Structure of the HP 8481A thermocouple chip.

The 8481A thermocouple consists of a silicon chip with several other materials deposited on top as shown in **Figure 3-3.** Each chip actually contains two thermocouples but this discussion will concentrate on only one for a moment. The tantalum-nitride resistor, for converting the rf energy into heat, is deposited on top of the silicon. A silicon-dioxide insulating layer separates the resistor from the silicon. At one end of the resistor, the end near the center of the chip, the insulating layer has a hole through which the resistor is connected to the silicon. The other edge of the resistor and the far edge of the silicon chip have gold beam-lead contacts. The beam leads not only make electrical contact to the external circuits, but also provide mounting surfaces for attaching the chip to a substrate, and serve as thermal paths for conducting heat away from the chip.

As the resistor converts the rf energy into heat, the center of the chip, which is very thin, gets hotter than the outside edge for two reasons. First, the shape of the

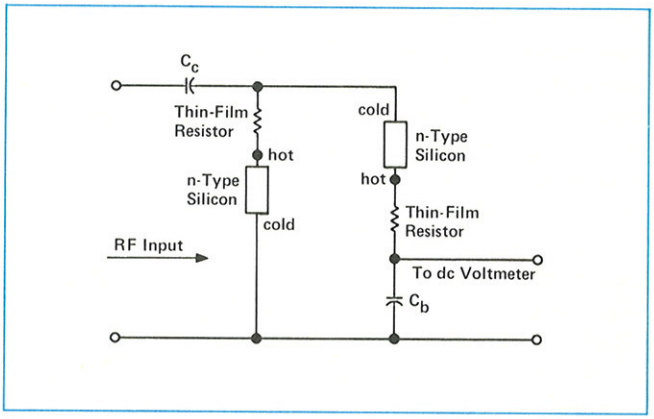

Figure 3-4. Schematic diagram of the HP 8481A thermocouple power sensor.

resistor causes the current density and the heat generated to be largest at the chip center. Second, the outside edges of the chip are thick and well cooled by conduction through the beam leads. Thus there is a thermal gradient across the chip which gives rise to the thermoelectric emf. The hot junction is the resistor-silicon connection at the center of the chip. The cold junction is formed by the outside edges of the silicon chip and the resistor. The cold junction is separated to form the two contacts to external circuitry.

The HP 8481A Power Sensor contains two identical thermocouples on one chip, electrically connected as in **Figure 3-4.** The thermocouples are connected in series

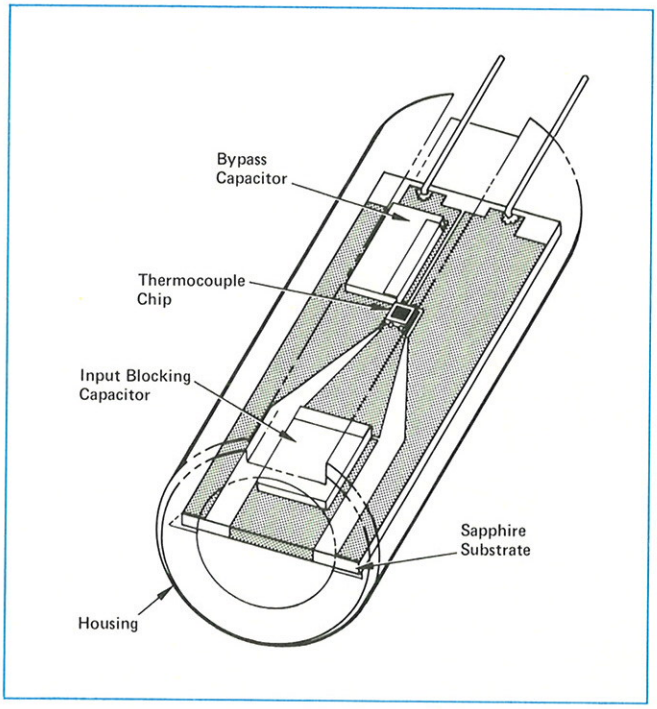

Figure 3-5. Sketch of the thermocouple assembly for the HP 8481A.

as far as the dc voltmeter is concerned. For rf frequencies, the two thermocouples are in parallel, being driven through coupling capacitor C_c. Half the rf current flows through each thermocouple. Each thin-film resistor and the silicon in series with it has a total resistance of 100 ohms. The two thermocouples in parallel form a 50 ohm termination for the rf transmission line. The lower node of the left thermocouple is directly connected to ground and the lower node of the right thermocouple is at rf ground through bypass capacitor C_b. The dc voltages generated by the separate thermocouples add in series to form a higher dc output voltage. The principal advantage, however, of the two thermocouple scheme is that both leads to the voltmeter are at rf ground; there is no need for an rf choke in the upper lead. If a choke were needed it would limit the frequency range of the sensor.

The thermocouple chip is attached to a transmission line deposited on a sapphire substrate as shown in **Figure 3-5.** Coplanar transmission line is used to allow the line dimensions to taper down to the chip size, while still maintaining the same characteristic impedance in every cross-sectional plane. This structure contributes to the very low reflection coefficient of the 8481A sensor, especially at microwave frequencies.

The principal characteristic of a thermocouple sensor for high frequency power measurement is the sensitivity in microvolts output per milliwatt of rf power input. The sensitivity is equal to the product of two other parameters of the thermocouple, the thermoelectric power and the thermal resistance.

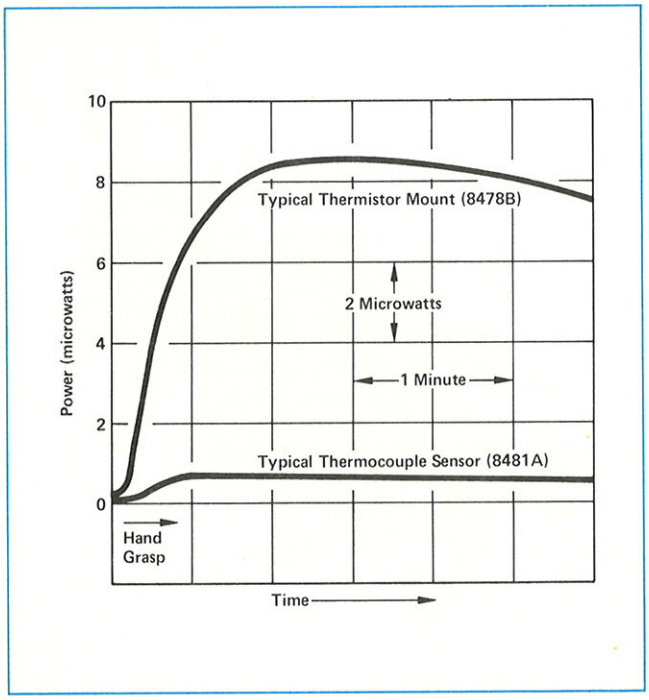

Figure 3-6. Zero drift of thermocouple and thermistor power sensors due to being grasped by a hand.

The thermoelectric power (not really a power but physics texts use that term) is the thermocouple output in microvolts per degree centigrade of temperature difference between the hot and cold junction. In the HP 8481A thermocouple mount, the thermoelectric power is designed to be 250 μV/°C. This is controlled by controlling the density of n-type impurities in the silicon chip.

The thickness of the HP 8481A silicon chip was selected so the thermocouple has a thermal resistance 0.4°C/mW. Thus the overall sensitivity of each thermocouple is 100 μV/mW. Two thermocouples in series, however, yield a sensitivity of only 160 μV/mW because of coupling between the thermocouples; the cold junction of one thermocouple is heated by the resistor of the other thermocouple giving a somewhat smaller temperature gradient.

The thermoelectric voltage is almost constant with temperature. It depends mainly on the temperature gradients and only slightly on the ambient temperature. Still, ambient temperature variations must be prevented from establishing gradients. The chip itself is only 0.8 mm long and is thermally short-circuited by the relatively massive sapphire substrate. The entire assembly is enclosed in a copper housing. **Figure 3-6** depicts the better thermal behavior of a thermocouple compared to a thermistor power sensor.

The thermoelectric power is not exactly constant, but does vary somewhat with temperature. At large powers, where the average thermocouple temperature is raised, the output voltage is larger than predicted by extrapolating data from low power levels. At a power level of 30 mW the output is 3 percent high, at 100 mW it is about 10 percent high. The circuitry in the HP power meters used with thermocouples compensates for this effect. Circuitry in the sensor itself compensates for changes in ambient temperature.

The thermal resistance limits the maximum power that can be dissipated. If the hot junction rises to 500°C, differential thermal expansion causes the chip to fracture. The HP 8481A is limited to 300 mW maximum average power.

The thermal resistance combines with the thermal capacity to form the thermal time constant of 120 microseconds. This means that the thermocouple voltage falls to within 37 percent of its final value 120 μs after the rf power is removed. The response time for measurements, however, is usually much longer because it is limited by noise considerations in the voltmeter circuitry.

The only significant aging mechanism found so far is thermal aging of the tantalum nitride. A group of devices were stress tested, producing the results of **Figure 3-7.** These curves predict that, if a device is left at 300 mW for one year, the resistance should increase by about 3.5 percent. Nine days at a half watt would cause an increase in resistance of 2 percent. The aging accumulates.

With such a design it is relatively easy to adapt the basic design to other requirements. It is easy, for example, to change each tantalum-nitride resistor to 150 ohms so that the thermocouple can work in 75 ohm systems. It is also easy to enhance low frequency performance by using larger blocking and bypass capacitors. This usually compromises high frequency performance due to increased loss and parasitic reactance of the capacitors. The low frequency HP 8482A Power Sensor is designed for 100 kHz to 4.2 GHz operation in contrast to the 8481A which operates from 10 MHz to 18 GHz.

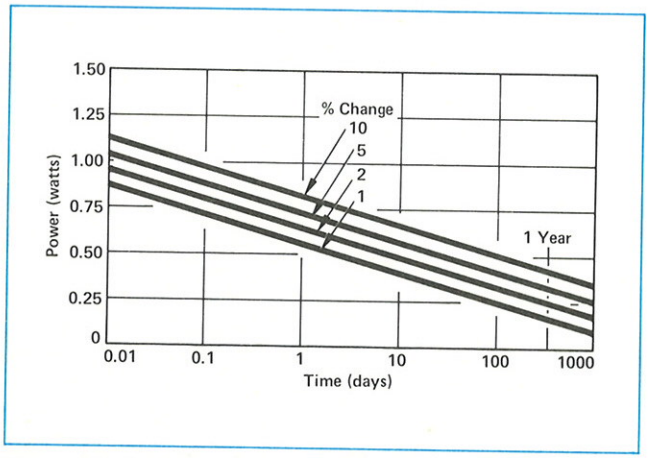

Figure 3-7. Results of step stress aging test show percent change in thermocouple resistance when left at various power levels continuously for various periods of time .

Power Meters for Modern Sensors

Design contributions do not stop at the sensing element itself or with the rf structure. The HP 435A Power Meter will be used to describe the basic instrumentation **(Figure 3-8).** This meter has full scale ranges from −25 dBm to +20 dBm for use with the 8481A. With other sensors the same dynamic range is translated up or down. With the semiconductor diode 8484A Power Sensor, to be described in the next chapter, the full scale ranges go from −65 dBm to −20 dBm.

The thermocouple dc output is very low-level (approximately 160 nV for 1 microwatt applied power), so it is difficult to transmit on an ordinary cable. Small, undesired thermocouple effects creep into the system—especially at connections and points of wear and corrosion. This problem is multiplied if the user wants a long cable between his sensor and power meter. For this reason it was decided to include the low-level dc circuitry in the power sensor, so only relatively high-level signals appear on the cable.

The only practical way to handle such low dc voltages is to "chop" them to form a square wave, amplify this with an ac-coupled system, then synchronously detect the high-level ac. For reasons mentioned above, it was decided to include the chopper and part of the first ac amplifier in the power sensor. The chopper itself

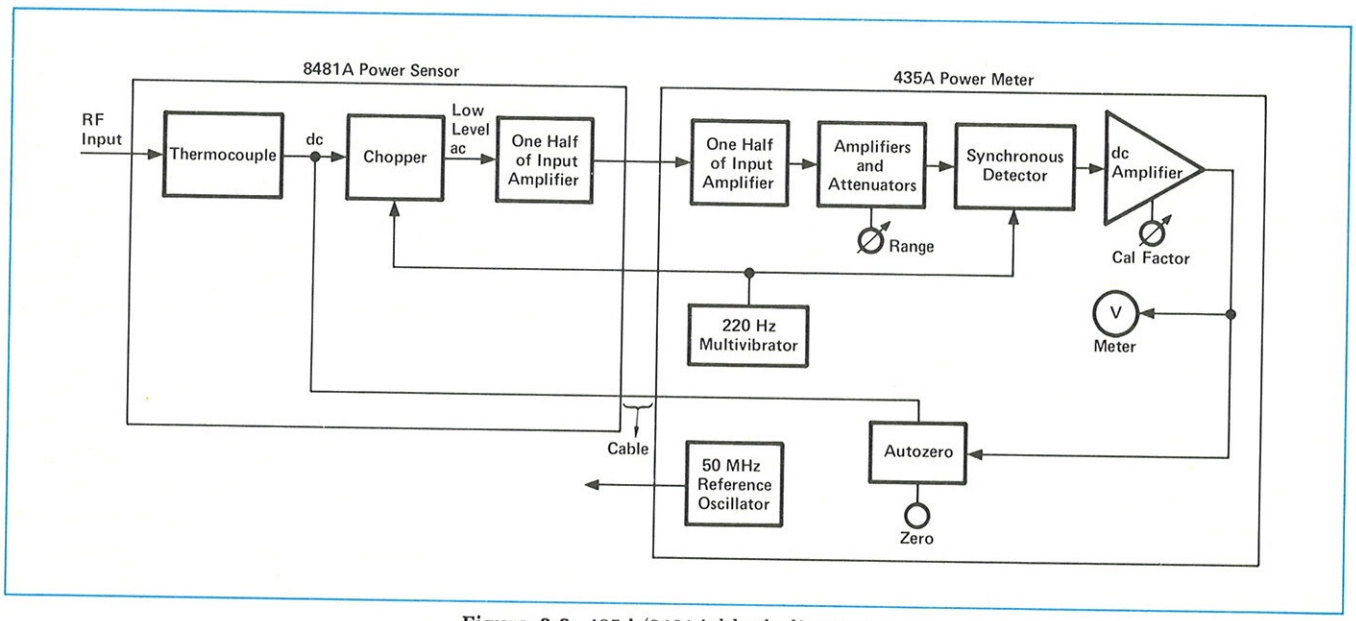

Figure 3-8. 435A/8481A block diagram.

(Figure 3-9) uses FET switches that are in intimate thermal contact. This is essential to keep the two FET's at exactly the same temperature to minimize drift. To eliminate undesired thermocouples only one metal, gold, is used throughout the entire dc path. All these contributions were necessary to help achieve the low drift already shown in **Figure 3-6.**

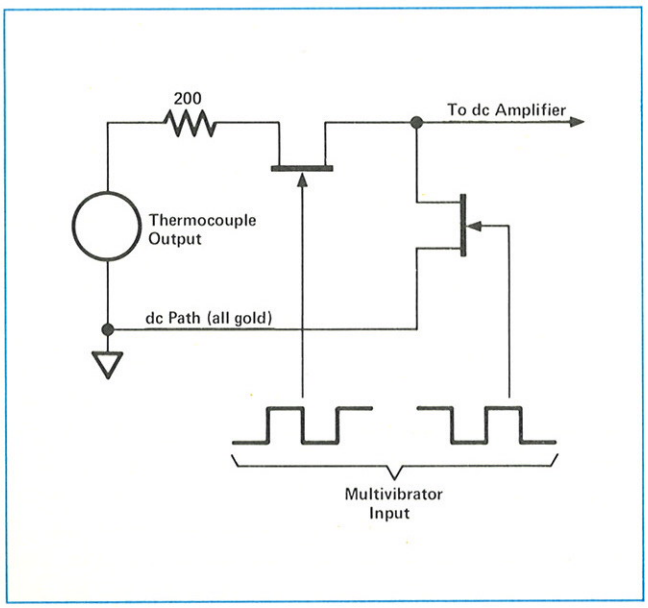

Figure 3-9. Simplified Schematic of chopper amplifier.

The chopping frequency is chosen at 220 Hz as a result of several factors. Factors that tend to dictate a high chopping frequency include lower 1/f noise and a larger possible bandwidth. Limiting the chopping to a low frequency is the fact that small spikes from chopping inevitably get included with the main signal. These spikes are at just the proper rate to be integrated by the synchronous detector and masquerade as valid signal. The fewer spikes per second, the smaller this masquerading signal. Since the spikes are also present during the zero-setting operation, and remain the same value during the measurement of a signal, the spikes are essentially removed from the meter indication by zero-setting and cause no error. The spikes do, however, use up dynamic range of the amplifiers.

One way to minimize noise while amplifying small signals is to limit the bandwidth. Since the noise generating mechanisms are broadband, limiting the amplifier bandwidth reduces the total noise power. The narrowest bandwidth is used for the weakest signals. As the power meter is switched to higher ranges the bandwidth increases so that measurements can be made more rapidly. On the most sensitive range the time constant is roughly 2 seconds while on the higher ranges the time constant is 0.1 seconds. A 2-second time constant corresponds to a 0 to 99 percent rise time of about 10 seconds.

Reference Oscillator

A frequent, sometimes well-directed, criticism of thermocouple power measurements is that such measurements are open-loop, and that thermistor power measurements are inherently more accurate. The increased confidence in the thermistor measurements results from the direct substitution of dc power for rf power in a closed-loop system. The bridge feedback of substituted dc power compensates for differences between thermistor mounts and for drift in the thermistor resistance–power characteristic without recalibration. With thermocouples, where there is no direct substitution, sensitivity differences between sensors or drift in the sensitivity of a sensor means a different dc output voltage for the same rf power. Because there is no feedback to correct for different sensitivities, measurements with thermocouple sensors are said to be open-loop.

The 435A solves this problem by including a 50 MHz power-reference oscillator whose output power is controlled very accurately. To verify the accuracy of the system, or adjust for a sensor of different sensitivity, the user connects his thermocouple sensor to the power-reference output and, using a front-panel screwdriver adjustment, sets his 435A to read 1.00 mW. The reference oscillator is applied to the input port of the power sensor just like the rf to be measured; the same capacitors and conductors are used in the same way for measurement and for calibration adjustment. This feature effectively transforms the system to a closed-loop, substitution-type system.

Automatic Measurements

The introduction of the modern thermocouple sensor corresponded in time with a demand for automatic measurements. This demand not only required a digital output of the power level being sensed, but complete digital control of the power meter as well as regular front panel control. This control had to include the ability to zero-set, to change ranges, and to indicate the units of power (e.g., mW, dBm, etc.). The HP 436A Power Meter was designed especially for this purpose.

The analog portion of the 436A is very similar to the 435A discussed in the previous section. The two instruments use the same power sensors, amplify the small dc voltages from the sensor by first chopping at a 220 Hz rate, then amplifying that ac signal, and synchronously detecting the ac signal just before metering. The synchronous detector is different to enable automatic measurements at the highest speed practical for rapid data gathering.

The heart of the 436A Power Meter is a patented logarithmic analog-to-digital converter **(Figure 3-10).** This circuit, as distinguished from the usual dual slope technique popular in digital voltmeters, allows readings in watts or dBm with the same accuracy and with a minimum of extra circuitry. Unlike analog approaches to the problem of log conversion, no warmup time is required and there is very little temperature drift (<0.001 dB/°C).

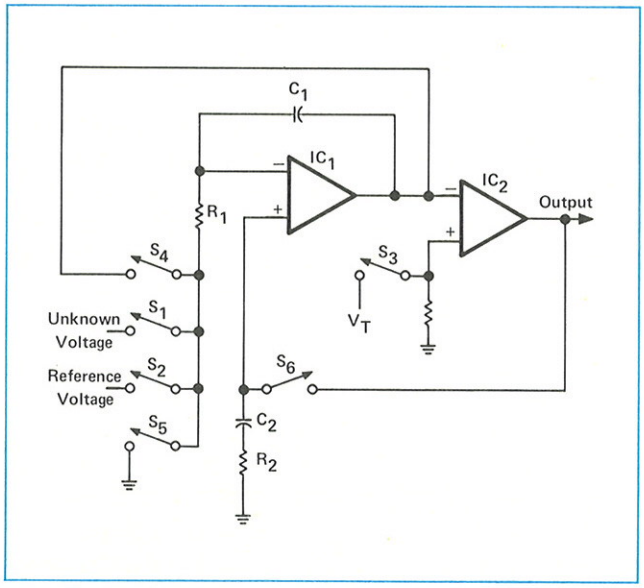

Figure 3-10. Simplified diagram of the analog to digital converter of the HP 436A.

At the start of the measurement cycle switch S_1 closes and connects the unknown to the integrator IC_1. After a fixed period of time switch S_1 opens leaving a voltage V_1 on the output of the integrator which is proportional to the unknown input voltage and hence the input power.

In the watts mode an appropriate reference voltage is connected to the integrator, through switch S_2, to discharge the integrator at a constant rate. The discharge continues until comparator IC_2 detects a zero crossing. The discharge time T is proportional to V_1 and hence to the unknown input voltage. The time is counted to get a digital result representing watts of input power.

In the log conversion mode the first part of the conversion cycle is the same so that voltage V_1 is on the integrator when switch S_1 opens. Then switches S_3 and S_4 are closed so that the capacitor C_1, initially charged to V_1, discharges exponentially through R_1 according to

$$v_o(t) = V_1 e^{-\frac{t}{R_1 C_1}} \qquad (3\text{-}1)$$

where $v_0(t)$ is the discharging output voltage on C_1. The discharge continues until $v_0(t)$ reaches threshold V_T, as sensed by the comparator. The time lapse T is given by

$$\frac{T}{R_1 C_1} = \ln \frac{V_1}{V_T} = 2.303 \log \frac{V_1}{V_T} \qquad (3\text{-}2)$$

The discharge time, or the time registered on the counter, is seen to be proportional to the log of V_1. R_1 and V_T are adjusted at the factory to provide precise conversion to dBm.

At the end of the measurement cycle, switches S_5 and S_6 are closed and a feedback loop is formed that places a charge on C_2 to remove any remaining voltage from IC_1.

Digital counters normally have an output uncertainty of ± one count. This is due to the internal time-base oscillator being out of synchronism with the start of the measurement interval by, at most, one count and also being out of sync with the end of the measurement by, at most, one count. Thus there is a maximum possible total uncertainty of two counts or ± one count. The analog-to-digital converter described here only has an ambiguity at the end of the measurement cycle. The beginning of the discharge cycle is triggered by the internal time base and therefore has no ambiguity. Thus the ambiguity in output indication is a total spread of one count or ± one-half count.

The HP 436A automatic power meter is capable of working with several different thermocouple mounts covering different power ranges and also of working with a diode detector power sensor (discussed in the next chapter). Each power sensor contains a resistor that indicates to the power meter the sensitivity of the sensor. With this resistor the 436A Power Meter can determine the mount sensitivity and adjusts the output indication appropriately.

In summary, the thin-film, semiconductor, thermocouple power sensor, because of its low reflection coefficient, can yield the most accurate, broad-range measurement system. When used with a modern digital power meter, fast and automated measurements are also possible.

IV. Diode Detector Power Sensors and Instrumentation

Rectifying diodes have long been used as detectors and for relative measurements at microwave frequencies. For absolute power measurement, however, their use has been limited mainly to the radio and the low microwave frequencies and to power levels already covered by thermistors and thermocouples. The high-frequency diodes have been of the point-contact variety and consequently fragile, not very repeatable, and subject to change with time. Now it is possible to construct metal-semiconductor junction diodes for microwave frequencies that are very rugged and consistent from diode to diode. These new diodes can measure power as low as −70 dBm (100 pW) to frequencies of at least 18 GHz. This chapter reviews the design of this detecting diode as a power sensor.

The same power meters used with thermocouple sensors, can be used for diode type power sensors because the electronic circuits for the two sensors have the same basic goals. First, voltages on the order of 100 nV are to be measured—so the same choppers, ac amplifiers, and synchronous detectors are needed. Second, power measurements with both kinds of sensors need a power-reference oscillator, with a precisely known power output, to adjust the calibration of the power meter to fit the particular sensor being used.

Diode Detector Principles

Diodes convert high frequency energy to dc because of their rectification properties, which arise from the non-linear current-voltage characteristic. It might seem that the ordinary silicon p-n junction diode would, when suitably packaged, be a sensitive detector. The basic problem with the silicon p-n diode is that, without bias, the diode has extremely high impedance and will supply little detected power to a load. An rf signal would have to be quite large to swing the junction voltage up to 0.7 volts where significant current begins to flow. One alternative is that the diode may be dc biased to 0.7 volts, then only a small rf signal causes significant rectified current. This effort turns out to be in vain, however, mainly because the forward bias gives rise to large amounts of noise and thermal drift. There is little, if any, improvement in the minimum power that can be metered.

A detecting diode ideally obeys the diode equation

$$i = I_s (e^{\alpha v} - 1) \qquad (4\text{-}1)$$

where i is the diode current, v is the net voltage across the diode, I_s is the saturation current and is constant at a given temperature, and α is a shortened form of writing q/nKT. K is Boltzmann's constant, T is absolute temperature, q is the charge of an electron and n is a correction constant to fit experimental data (its value turns out to be about 1.1 for the devices used here for sensing power). The value of α is typically a little under 40 (volts^{-1}). Equation (4-1) is often written as the power series

$$i = I_s \left(\alpha v + \frac{(\alpha v)^2}{2!} + \frac{(\alpha v)^3}{3!} + \cdots\right) \qquad (4\text{-}2)$$

It is the second and other even-order terms of this series which provide the rectification. For small signals only the second-order term is significant so the diode is said to be operating in the square-law region. When v is so high that the fourth and higher order terms become significant the diode is no longer square law.

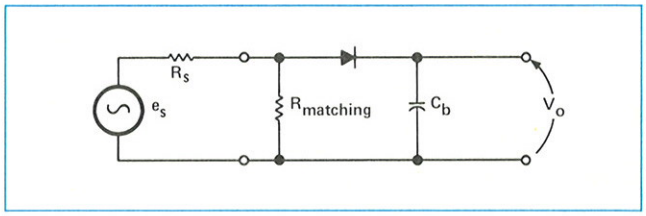

Figure 4-1. Circuit diagram of a source and a diode detector with matching resistor.

The simplified circuit of **Figure 4-1** represents an unbiased diode detector for detecting low level, rf signals. Maximum power is transferred to the diode when the diode resistance for small rf voltages is matched to the source resistance. The diode resistance at the origin, found by differentiating (4-1), is

$$R_o = \frac{1}{\alpha I_s} \qquad (4\text{-}3)$$

Resistance R_o is a strong function of temperature; this means the diode sensitivity and the reflection coefficient are also strong functions of temperature. To achieve less temperature dependence, R_o is much larger than the source resistance and a 50 ohm matching resistor is included to terminate the generator. If R_o, when substituted for the diode of **Figure 4-1,** were made too large, however, there would be poor power conversion from rf to dc; thus, larger R_o yields decreased sensitivity. A compromise between good sensitivity to small signals and good temperature performance results from making I_s about 10 microamps and R_o about 2.5 K ohms.

The desired value of leakage current I_s can be achieved by constructing the diode of suitable materials that have a low potential barrier across the junction.

Metal-semiconductor junctions, called Schottky diodes, can be designed for such a low-barrier potential. The traditional point-contact diode formed a metal-semiconductor or Schottky junction. Due to the way they are built, however, point-contact diodes are inherently fragile: mechanically due to whisker movement, and electrically due to the very small junction area resulting in high current densities and local hot spots. Besides the fragile nature of point contacts, origin resistance R_o and junction capacitance C_o are quite variable from diode to diode. The junction capacitance and other parasitic reactances must be kept small in order to achieve frequency independent performance.

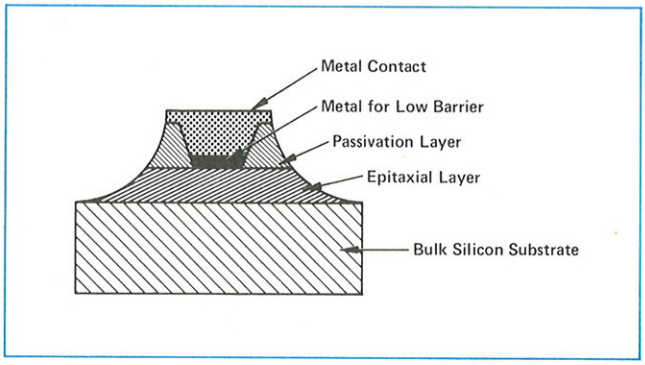

Figure 4-2. The structure of a photometallurgically built low-barrier Schottky diode.

Junction diodes of the low-barrier Schottky variety and with low enough junction capacitance for good performance to 18 GHz can be built with photometallurgical techniques **(Figure 4-2).** A thin, lightly-doped epitaxial layer is grown atop a heavily-doped, monocrystalline silicon substrate. The surface of the epitaxial layer is oxidized to form a protective, insulating layer called the passivation layer. A hole is then etched in the oxide, and a suitable metal is deposited to form a junction with the epitaxial layer. The result is a Schottky diode. The choice of metal controls the barrier height and therefore the high saturation current and low origin resistance so important for good performance. A low capacitance of about 0.1 pF is achieved by keeping the metal-semiconductor junction small and by etching the chip into a mesa-type shape.

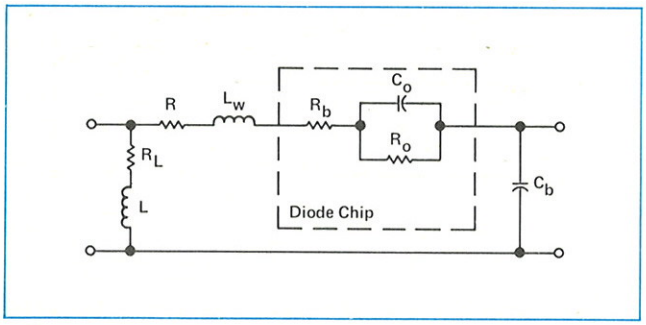

Figure 4-3. The rf circuit associated with a low-barrier Schottky diode power sensor.

Such a low-barrier Schottky diode (LBSD) is included in the HP 8484A Power Sensor which covers the 10 MHz to 18 GHz frequency range and can measure power from −20 dBm (10 μW) to −70 dBm (100 pW). To achieve such frequency independent performance, other rf circuit elements must be included to compensate for the inevitable parasitic reactances associated with the diode, its connections, and the dc circuitry.

The equivalent circuit for the rf portion of the HP 8484A Power Sensor is shown in **Figure 4-3.** The diode chip itself has three elements: R_o is the origin resistance of the junction; C_o is the junction capacitance; and R_b is the bulk resistance of the semiconductor material. C_b is the bypass capacitor used also as a low-pass filter to integrate the current through the diode. L_w is the inductance associated with the bonding wires to the diode. Resistor R is about 30 ohms and intentionally added to increase the loss of the resonance of L_w with the capacitors. This loss makes the resonance of such low Q that it is not noticeable. Resistor R_L is the terminating resistance for the transmission line. L is actually a short section of transmission line that compensates for other reactances to yield an overall flat performance with frequency. The rf circuitry, including the 50 ohm termination, is constructed on a sapphire substrate using thin-film techniques.

Diode Mount for Sensing Power

The advantage of the low-barrier Schottky diode over thermocouple power sensors, is that the detecting diode is some 3000 times more efficient in converting rf power to dc. In measuring power levels of 100 picowatts (−70 dBm) the diode detector output is about 50 nanovolts. This low signal level requires careful design to prevent leakage signals and thermocouple effects from dominating the desired signal (see **Figure 4-4).** The HP 8484A Power Sensor has gold leads from the diode to a chopper-amplifier. The chopper-amplifier, which presents a 5 K ohm load impedance to the diode, is somewhat different than for the thermocouple sensors, even though the power meter itself is the same for both types of sensors.

The major thermal drift mechanism, the one that dominated the design of the diode mount, is the thermal emf generated by any temperature gradient that appears across the diode. The mechanical design of the 8484A **(Figure 4-4)** minimized this gradient by insulating the diode package and arranging the thermal paths so the primary heat source is at the rf input connector. Any

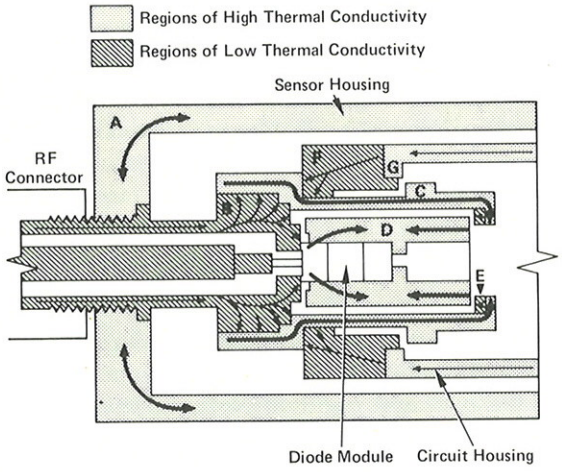

Figure 4-4. Sensor housing is designed for low thermal drift. In the drawing, housing A acts as a sink for heat from the rf connector or as a source for heat caused by handling. Low-conductivity region B delivers heat to one end of the diode module, and to high-conductivity region C, which transfers it to the opposite end of the module. High-conductivity region D distributes the heat from B and C uniformly. Region E balances the heat from C to D with that from B to D. Region F blocks heat transfer from circuit housing G.

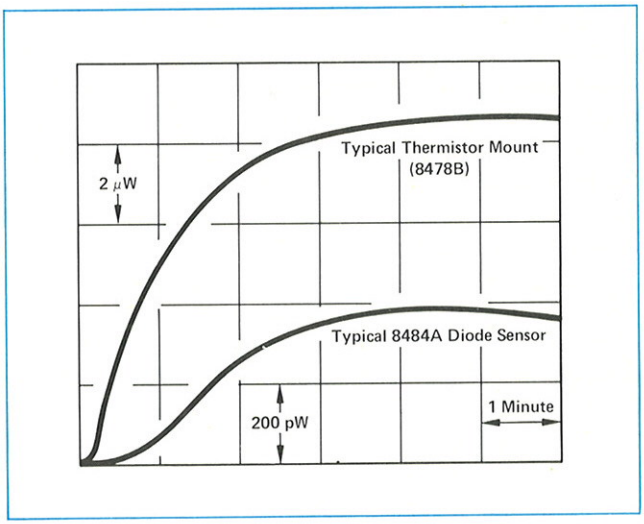

Figure 4-5. Drift of a typical 8484A Power Sensor in response to a hand grasp, compared with that of a typical thermistor power sensor. Both sensors were on their most sensitive ranges, which differ by 10^4 in sensitivity.

heat that does enter the diode area is directed uniformly to both ends of the diode package. With both ends changing temperature uniformly, the temperature gradient across the diode is almost nil, thus minimizing drift. Any thermal gradient is also reduced by the heat sinking action of the outer housing (see **Figure 4-5).**

Like other Hewlett-Packard power sensors, the 8484A is supplied with calibration factor vs. frequency data. Diode detectors sometimes have calibration factors at microwave frequencies that are larger than those at 50 MHz. This means that the calibration factor dial on the power meter should be adjusted to the proper 50 MHz value before going through the calibration adjustment procedure for open-loop power measurements. The reference calibration factor is clearly marked on each 8484A Power Sensor.

The power emerging from the 50 MHz reference output on the power meters is 1 mW (0 dBm), which is near the center of the dynamic range of most power sensors, but outside the range of the sensitive 8484A. Since the range of any power sensor may be translated upward by a suitable attenuator, a special attenuator of 30 dB at 50 MHz is supplied with each 8484A. When that attenuator is attached to the power reference output terminal on the power meter, the emerging power is 1 microwatt (−30 dBm). Attenuator design is such that a maximum error of 1 percent is added to the calibration step.

The sensitivity of the diode detector in the 8484A is somewhat influenced by ambient temperature. Compensation circuitry is included in the sensor, but, at extreme ambient temperatures, the instrument should be recalibrated using the reference oscillator and the 30 dB attenuator to obtain the most accurate results. Typical sensitivity variations with temperature for uncompensated and compensated detectors are shown in **Figure 4-6.**

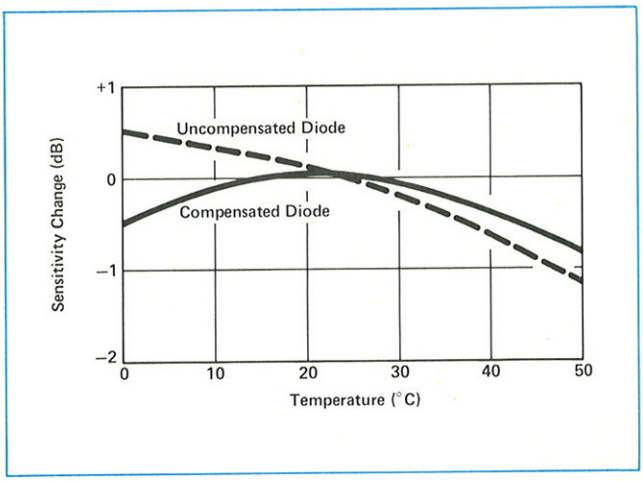

Figure 4-6. Typical sensitivity variations with ambient temperature for compensated (8484A) and uncompensated diode sensors.

The 8484A power sensor can accept average and peak overloads of 200 mW (+23 dBm) without permanent damage. The maximum level for accurate measurement, limited by the diode square-law region, is 0.01 mW (−20 dBm). This results in a safety range of 20,000:1 (43 dB).

Amplitude Modulation

There is a somewhat popular, but erroneous opinion that diode detectors cannot measure the average power of an amplitude modulated wave. This results from the concept of a diode detector as a peak detector. Proponents of this belief say that only sensors that convert energy to another form, such as a thermocouple or thermistor that measures heat, actually measure the true average power. In actuality, diode detectors do properly measure average power so long as operation is confined to their square-law region. This can be verified experimentally by measuring amplitude modulated waves with thermocouples and then with diode detectors. The validity can also be demonstrated by a mathematical analysis of equation (4-1) in the circuit of **Figure 4-1.** Such an analysis is beyond the scope of this application note.

The erroneous belief about the diode detector arises from mistakenly applying the principle of peak detectors. The principle of the peak detector is that voltage stored on bypass capacitor C_b of **Figure 4-1** during the peaks of the modulation cycle is quite large. It is so large that, in the valleys of the modulation cycle, the rf peaks are not large enough to switch the diode into conduction. There is no measurement of power level in the valley because the rf source is effectively disconnected from the voltmeter by the back-biased diode.

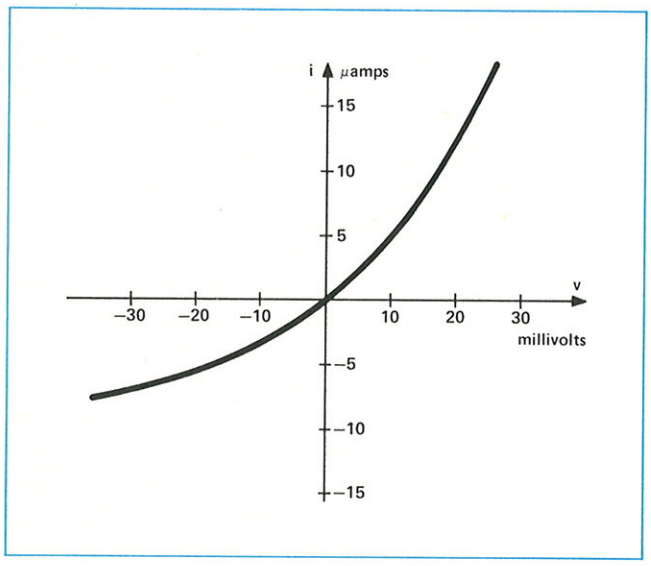

Figure 4-7. The square-law portion of the i-v characteristic for a typical low-barrier Schottky diode.

Figure 4-7 shows the square-law range of the i-v characteristic for a typical low-barrier Schottky diode. If there is −20 dBm of CW power applied to the circuit of **Figure 4-1** that i-v characteristic is traversed every rf cycle. The voltage across the diode swings from about −35 mV to +25 mV. The capacitor C_b is charged to about 5 mV and supplies 1 μa of dc current to the voltmeter amplifier. The average source impedance that charges C_b is about 2.5 K ohms as found from the slope of the i-v characteristic at v = −5 mV.

Now if the rf amplitude is reduced by 20 dB to −40 dBm, the voltage across the diode swings only ±3 mV, at first about the −5 mV position but eventually about the 0.05 mV position. Note, however, that the diode impedance is still about 2.5 K ohms during every portion of the rf cycle. The diode is never "off"; it never disconnects C_b from the rf source. In summary, the diode is just as efficient in discharging C_b during valleys of the amplitude modulated signal as it is in charging C_b during crests of the amplitude modulated signal. Only when rf voltage levels are so large that the average diode resistance during crests is significantly different than during valleys of the modulating signal is the peak detector "on-off concept" valid.

Diodes can, in principle, be used for absolute power measurements outside the square-law region by using appropriate shaping or non-linear amplification. Such shaping, however, is only valid for CW and constant amplitude waveforms. For general amplitude modulation, shaping is invalid. Even for CW waveforms, the shaping required for accurate measurement is likely to be a strong function of temperature.

The principal advantage of the low-barrier Schottky diode is the ability to measure power levels down to 100 picowatts (−70 dBm) from 10 MHz to 18 GHz. This level is about 30 dB (1000:1) lower than the power levels needed by the crystal radios from the early days of electronics. The sensitivity at low levels is achieved while maintaining a low-reflection coefficient and therefore also maintaining accurate, convenient power measurements.

V. Mismatch Errors

In almost all rf and microwave measurements there are many possible errors. In power measurements the largest errors are almost always caused by mismatch. These errors, which have several aspects, are quite complicated and are seldom completely understood or properly evaluated. This chapter concentrates on errors associated with mismatch. Other errors are assumed to be nonexistent; that is, the power meter is considered to be perfectly accurate. Chapter VI considers the other errors involved in power measurements and the combination of all errors.

The goal of an absolute power measurement is to characterize the power output from some source (generator). Sometimes the generator is an actual signal generator or oscillator where the power sensor is attached directly to the generator. On other occasions, however, the generator is actually an equivalent generator. The power source is separated from the measurement point by such components as transmission lines, directional couplers, amplifiers, mixers, etc. All those components are considered as parts of the generator. The port that the power sensor is connected to, is also the output port of the equivalent generator.

In order to analyze the effects of mismatch this chapter explains ways to describe loads, including power sensors, and generators that apply to the rf and microwave frequency ranges. The microwave descriptions are related back to the equivalent low-frequency concepts for those familiar with those frequencies. Power flow between an arbitrary generator and load is then analyzed. From that analysis the terms mismatch loss and mismatch uncertainty are defined.

RF Circuit Descriptions

At low frequencies methods for describing a generator include the Thevenin and Norton equivalent circuits. The Thevenin equivalent circuit of a generator, for example, has a voltage generator e_s in series with an impedance Z_g as shown in **Figure 5-1.** For a generator, even if composed of many components, e_s is defined as the voltage across the output port when the load is an open circuit. Z_g is defined as the impedance seen looking back into the generator while all the sources inside the generator are reduced to zero.

The power delivered by a generator to a load is a function of the load impedance. If the load is a perfect open or short circuit, the power delivered is zero. Analysis of **Figure 5-1** would show that the power delivered to the load is a maximum when load impedance Z_ℓ is the complex conjugate of the generator impedance Z_g. This power level is called the "power available from a generator," or "maximum available power," or "available power." When $Z_\ell = (R_\ell + jX_\ell)$ and $Z_g = (R_g + jX_g)$ are complex conjugates of each other, their resistive parts are equal and their imaginary parts are identical in magnitude but of opposite sign; thus $R_\ell = R_g$ and and $X_\ell = -X_g$. Complex conjugate is written with an * so that $Z_\ell = Z_g^*$ is the required relationship for maximum power transfer.

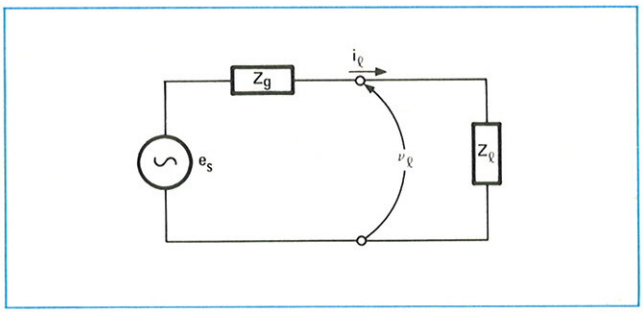

Figure 5-1. A Thevenin equivalent generator connected to an arbitrary load.

The Thevenin equivalent circuit is not very useful at microwave frequencies for a number of reasons. One reason is that the open circuit voltage is difficult to measure because of fringing capacitance and the loading effect of a voltmeter probe. Furthermore, the concept of voltage loses usefulness at microwave frequencies where it is desired to define the voltage between two points separated by a significant fraction of a wavelength. Consider the problems involved in discussing voltage in rectangular waveguide. As a result, power is much more frequently used than voltage for characterizing generators at rf and microwave frequencies.

The open circuit that defines the Thevenin equivalent voltage generator is useless for measuring power because the power dissipated in an open is always zero. The reference impedance that is used for characterizing rf generators is almost always 50 ohms. The reason for this is that 50 ohms is easy to simulate over the entire frequency range of interest with a transmission line of 50 ohms characteristic impedance and with a reflectionless termination. The standard symbol for characteristic impedance, Z_o, is also the standard symbol for reference impedance. In some cases, where, for example, 75 ohm transmission lines are used in systems with a 50 ohm reference impedance, another symbol, such as Z_r, should be used for reference impedance. Z_o will be used in this application note to mean reference impedance. A generator is characterized, therefore, by the power it delivers to a reference load Z_o (=50 ohms). In general, that power is not equal to the maximum available power from the generator; they are equal only if $Z_g = Z_o$.

As frequencies approach the microwave spectrum, the concept of impedance, like that of voltage, loses usefulness and is replaced by reflection coefficient. The impedance seen looking down a transmission line toward a mismatched load, varies drastically with position along the line. The real part, the imaginary part, the magnitude, and the phase of impedance are all complicated functions of position. Reflection coefficient, soon to be defined, is well-behaved; reflection coefficient has a magnitude that is constant and a phase angle that varies linearly with distance from the load.

Reflection Coefficient

At microwave frequencies, where power typically is delivered to a load by a transmission line that is many wavelengths long, it is very convenient to replace the impedance description of the load, involving voltage and current and their ratio (Ohm's Law), with a reflection coefficient description involving incident and reflected traveling waves and their ratio. To characterize a passive load, Ohm's Law is replaced by

$$\frac{b_\ell}{a_\ell} = \Gamma_\ell \qquad (5\text{-}1)$$

where a_ℓ is proportional to the voltage of the incident wave, b_ℓ is proportional to the voltage of the reflected wave, and Γ_ℓ is defined to be the reflection coefficient of the load. All three quantities are, in general, complex numbers and change with frequency. The quantities a_ℓ and b_ℓ are normalized* in such a way that the following equations hold:

$$|a_\ell|^2 = P_i \qquad (5\text{-}2)$$

$$|b_\ell|^2 = P_r \qquad (5\text{-}3)$$

where P_i is power incident on the load and P_r is power reflected by it. The net power dissipated by the load, P_d, is given by

$$P_d = P_i - P_r = |a_\ell|^2 - |b_\ell|^2 \qquad (5\text{-}4)$$

This power is the total power used by the load; it includes power converted to heat, power radiated to space, and power that leaks through accessory cables to other pieces of equipment.

Transmission line theory relates the reflection coefficient, Γ_ℓ, of a load to its impedance, Z_ℓ, as follows:

$$\Gamma_\ell = \frac{Z_\ell - Z_o}{Z_\ell + Z_o} \qquad (5\text{-}5)$$

where Z_o is the characteristic impedance of the system. Further, the load voltage, v_ℓ, and load current, i_ℓ, are given by

$$v_\ell = \text{Incident voltage} + \text{reflected voltage} = \sqrt{Z_o}\,(a_\ell + b_\ell)$$

$$i_\ell = \text{Incident current} - \text{reflected current} = \frac{1}{\sqrt{Z_o}}\,(a_\ell - b_\ell)$$

since current in a traveling wave is obtained from the voltage by dividing by Z_o. Solving for a_ℓ and b_ℓ, we have

$$a_\ell = \frac{1}{2\sqrt{Z_o}}\,(v_\ell + Z_o i_\ell) \qquad (5\text{-}6)$$

$$b_\ell = \frac{1}{2\sqrt{Z_o}}\,(v_\ell - Z_o i_\ell) \qquad (5\text{-}7)$$

These equations are used in much of the literature to define a_ℓ and b_ℓ (see the reference by Kurakawa). The aim here, however, is to introduce a_ℓ and b_ℓ more intuitively. Although (5-6) and (5-7) appear complicated, the relationships to power (equations 5-2, 5-3, and 5-4) are very simple. The Superposition Theorem, used extensively for network analysis, applies to a_ℓ and b_ℓ; the Superposition Theorem does not apply to power.

Reflection coefficient Γ_ℓ is frequently expressed in terms of its magnitude ρ_ℓ and phase ϕ_ℓ. Thus ρ_ℓ gives the magnitude of b_ℓ with respect to a_ℓ and ϕ_ℓ gives the phase of b_ℓ with respect to a_ℓ.

The most common methods of measuring reflection coefficient Γ_ℓ involve observing a_ℓ and b_ℓ separately and then taking the ratio. Sometimes it is difficult to observe a_ℓ and b_ℓ separately, but it is possible to observe the interference pattern formed by a_ℓ and b_ℓ on a transmission line. This pattern is called the standing-wave pattern. The interference pattern has regions of maximum and of minimum signal strength. The maximums are formed by constructive interference between a_ℓ and b_ℓ and have amplitude $|a_\ell| + |b_\ell|$. The minimums are formed by destructive interference and have amplitude $|a_\ell| - |b_\ell|$. The ratio of the maximum to the minimum is called the Standing-Wave Ratio (SWR) and can be measured with a slotted line and moveable probe. SWR is related to the magnitude of reflection coefficient ρ_ℓ by

$$\text{SWR} = \frac{|a_\ell| + |b_\ell|}{|a_\ell| - |b_\ell|} = \frac{1 + |b_\ell / a_\ell|}{1 - |b_\ell / a_\ell|} = \frac{1 + \rho_\ell}{1 - \rho_\ell} \qquad (5\text{-}8)$$

A popular method of visualizing the flow of power through a component or among various components is by means of a flow diagram called a signal-flow graph.

* If the transmission line characteristic impedance is Z_o, the normalization factor is $\sqrt{Z_o}$; that is, a_ℓ is obtained from the voltage of the incident wave by dividing by $\sqrt{Z_o}$. Similarly, b_ℓ is obtained from the voltage of the reflected wave by dividing by $\sqrt{Z_o}$.

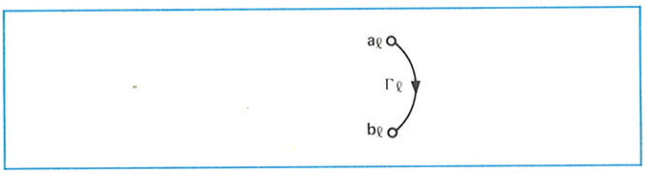

Figure 5-2. Signal-flow graph for a load.

The signal-flow graph for a load **(Figure 5-2)** has two nodes, one to represent the incident wave a_ℓ and the other to represent the reflected wave b_ℓ. They are connected by branch Γ_ℓ which shows how a_ℓ gets changed to become b_ℓ.

Microwave Generators

Just as the Thevenin equivalent had two quantities for characterizing a generator, generator impedance and open circuit voltage; the microwave equivalent has two quantities for characterizing a microwave or rf generator, Γ_g and b_s. The equation for a generator is

$$b_g = b_s + \Gamma_g a_g \qquad (5\text{-}9)$$

where:

- b_g is the wave emerging from the generator
- a_g is the wave incident upon the generator from other components
- Γ_g is the reflection coefficient looking back into the generator
- b_s is the internally generated wave

Γ_g is related to Z_g by

$$\Gamma_g = \frac{Z_g - Z_o}{Z_g + Z_o} \qquad (5\text{-}10)$$

which is very similar to (5-5). b_s is related to the power to a reference load from the generator, P_{gZo}, by

$$P_{gZo} = |b_s|^2 \qquad (5\text{-}11)$$

b_s is related to the Thevenin voltage e_s by

$$b_s = \frac{e_s \sqrt{Z_o}}{Z_o + Z_g} \qquad (5\text{-}12)$$

The signal-flow graph of a generator has two nodes representing the incident wave a_g and reflected wave b_g. The generator also has an internal node b_s that represents the ability of the generator to produce power. It contributes to output wave b_g by means of a branch of value one. The other component of b_g is that portion of the incident wave a_g, that is reflected off the generator.

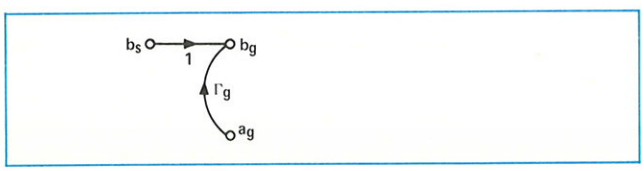

Figure 5-3. Signal-flow graph of a microwave generator.

Power Transfer

Now that equivalent circuits for a load and generator have been discussed, the flow of power from the generator to the load may be analyzed. When the load is connected to the generator, the emerging wave from the generator becomes the incident wave to the load and the reflected wave from the load becomes the incident wave to the generator. The complete signal-flow graph **(Figure 5-4)** shows the identity of those waves by connecting node b_g to a_ℓ and node b_ℓ to a_g with branches of value one.

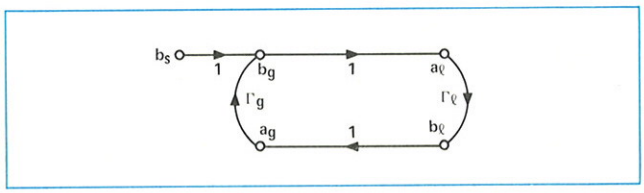

Figure 5-4. The complete signal-flow graph of a generator connected to a load.

Figure 5-4 shows the effect of mismatch or reflection. First, power from the generator is reflected by the load. That reflected power is re-reflected from the generator and combines with the power then being created by the generator, generating a new incident wave. The new incident wave reflects and the process continues on and on. It does converge, however, to the same result that will now be found by algebra.

The equation of the load (5-1) is rewritten with the identity of a_g to b_ℓ added as:

$$b_\ell = \Gamma_\ell a_\ell = a_g \qquad (5\text{-}13)$$

The equation of the generator (5-9) is also rewritten with the identity of a_ℓ to b_g added as:

$$b_g = b_s + \Gamma_g a_g = a_\ell \qquad (5\text{-}14)$$

Equations (5-13) and (5-14) may be solved for a_ℓ and b_ℓ in terms of b_s, Γ_ℓ and Γ_g

$$a_\ell = \frac{b_s}{1 - \Gamma_g \Gamma_\ell} \qquad (5\text{-}15)$$

$$b_\ell = \frac{b_s \Gamma_\ell}{1 - \Gamma_g \Gamma_\ell} \qquad (5\text{-}16)$$

From these solutions the incident and reflected powers can be calculated

$$P_i = |a_\ell|^2 = |b_s|^2 \frac{1}{|1 - \Gamma_g \Gamma_\ell|^2} \qquad (5\text{-}17)$$

$$P_r = |b_\ell|^2 = |b_s|^2 \frac{|\Gamma_\ell|^2}{|1 - \Gamma_g \Gamma_\ell|^2} \qquad (5\text{-}18)$$

Equation (5-17) gives the somewhat startling result that power flowing toward the load depends on the load.

The power dissipated, P_d, is equal to the net power delivered by the generator to the load, $P_{g\ell}$

$$P_d = P_{g\ell} = P_i - P_r = |b_s|^2 \frac{1 - |\Gamma_\ell|^2}{|1 - \Gamma_g \Gamma_\ell|^2} \quad (5\text{-}19)$$

Two particular cases of equation (5-19) are of interest. First, if Γ_ℓ were zero, that is if the load impedance were Z_o, (5-19) would give the power delivered by the generator to a Z_o load

$$P_{g\ell} \Big|_{Z_\ell = Z_o} = P_{gZo} = |b_s|^2 \quad (5\text{-}20)$$

This case is used to define b_s.

The second case of interest occurs when

$$\Gamma_g = \Gamma_\ell^* \quad (5\text{-}21)$$

where * indicates the complex conjugate. What (5-21) means in words is that the reflection coefficient looking toward the load from the generator is the complex conjugate of the reflection coefficient looking back toward the generator. It is also true that the impedances looking in the two directions are complex conjugates of each other. The generator is said to be "conjugately matched." If Γ_ℓ is somehow adjusted so that (5-21) holds, the generator puts out its "maximum power," P_{av}, which can be expressed as

$$P_{av} = \frac{|b_s|^2}{1 - |\Gamma_g|^2} \quad (5\text{-}22)$$

Comparing (5-20) and (5-22) shows that $P_{av} \geq P_{gZo}$.

Unfortunately, the term "match" is popularly used to describe both conditions, $Z_\ell = Z_o$ and $Z_\ell = Z_g^*$. The use of the single word "match" should be dropped in favor of "Z_o match" to describe a load of zero reflection coefficient, and in favor of "conjugate match" to describe the load that provides maximum power transfer.

Now the error can be plainly seen. When a power sensor is attached to a generator, $P_{g\ell}$ of equation (5-19) is measured. But the proper power for characterizing the generator is P_{gZo} of equation (5-20). The ratio of equations (5-20) to (5-19) is

$$\frac{P_{gZo}}{P_{g\ell}} = \frac{|1 - \Gamma_g \Gamma_\ell|^2}{1 - |\Gamma_\ell|^2} \quad (5\text{-}23)$$

or in dB

$$dB = 10 \log \frac{P_{gZo}}{P_{g\ell}} \quad (5\text{-}24)$$

$$= 10 \log |1 - \Gamma_g \Gamma_\ell|^2 - 10 \log (1 - |\Gamma_\ell|^2)$$

This ratio (in dB) is called the "Z_o mismatch loss." It is quite possible that (5-23) could yield a number less than one. Then (5-24) would yield a negative number of dB. In that case more power would be transferred to the particular load being used than to a Z_o load; the Z_o mismatch loss is actually a gain. An example of such a case occurs when the load and generator are conjugately matched.

A similar error exists for the case of conjugate match; the measurement of $P_{g\ell}$ from (5-19) differs from P_{av} of (5-22). The ratio of those equations is

$$\frac{P_{av}}{P_{g\ell}} = \frac{|1 - \Gamma_g \Gamma_\ell|^2}{(1 - |\Gamma_g|^2)(1 - |\Gamma_\ell|^2)} \quad (5\text{-}25)$$

or in dB

$$dB = 10 \log \frac{P_{av}}{P_{g\ell}} \quad (5\text{-}26)$$

$$= 10 \log |1 - \Gamma_\ell \Gamma_g|^2 - 10 \log (1 - |\Gamma_g|^2) - 10 \log (1 - |\Gamma_\ell|^2)$$

This ratio (in dB) is called the **conjugate mismatch loss.**

If Γ_ℓ and Γ_g were completely known, there would be no difficulty. The power meter reading of $P_{g\ell}$ would be combined with the proper values of Γ_ℓ and Γ_g in (5-23) or (5-25) to calculate P_{gZo} or P_{av}. The mismatch would be corrected and there would be no uncertainty.

Mismatch Uncertainty

Γ_ℓ and Γ_g are seldom completely known. Only the magnitudes ρ_ℓ and ρ_g, are usually measured or specified. In these cases, the first term of the right side of equations (5-24) and (5-26) cannot be exactly calculated because of the lack of phase information, but the maximum and minimum values can be found. The maximum and minimum values of $10 \log |1 - \Gamma_g \Gamma_\ell|^2$ are called "Mismatch Uncertainty Limits" and are given the symbol M_u. The maximum occurs when $\Gamma_\ell \Gamma_g$ combines with "one" in phase to yield

$$M_{u\,max} = 10 \log (1 + \rho_g \rho_\ell)^2 \quad (5\text{-}27)$$

This maximum limit will always be a positive number but it cannot be larger than 6 dB (this occurs when $\rho_\ell = \rho_g = 1$). The minimum value of the Mismatch Uncertainty occurs when $\Gamma_\ell \Gamma_g$ combines with "one" exactly out of phase to yield

$$M_{u\,min} = 10 \log (1 - \rho_g \rho_\ell)^2 \quad (5\text{-}28)$$

The minimum limit will always be a negative number. It is also true that the magnitude of the minimum limit will be greater than the magnitude of the maximum limit, but usually by a very small amount.

Sometimes the mismatch uncertainty limits are given in percent deviation from "one" rather than in dB. In this case

$$\%M_u = 100\,[(1 \pm \rho_g \rho_\ell)^2 - 1] \qquad (5\text{-}29)$$

Mismatch uncertainty limits can be calculated by substituting the values of ρ_ℓ and ρ_g into equations (5-27), (5-28), and (5-29). The current popularity of hand-held calculators with the log function makes this quite easy.

The mismatch uncertainty limits can be easily found by using the complimentary HP Reflectometer/ Mismatch Error Limits Calculator.* This calculator also has slide rule scales for converting between SWR and ρ as well as other scales. Instructions and examples are printed on the calculator.

Many programmable electronic calculators have a series of programs available especially suited for electrical engineering problems. One of the programs is often for calculating mismatch uncertainty limits, either in terms of SWR or of ρ. It is beyond the scope of this note to explain how each calculator accomplishes this; consult the specific calculator manuals.

Mismatch Loss

The second term on the right side of equation (5-24), $-10 \log (1 - |\Gamma_\ell|^2)$, is called mismatch loss. It accounts for the power reflected from the load. In power measurements, mismatch loss is usually taken into account when correcting for the Calibration Factor of the sensor. Calibration Factor, a single number that corrects for both the mismatch loss and the effective efficiency, is discussed in the next chapter.

The conjugate mismatch loss of equation (5-26) can be calculated, if needed. The uncertainty term is the same as the Z_o mismatch loss uncertainty term and the remaining terms are mismatch loss terms, one at the generator and one at the load. Conjugate mismatch loss is not used much anymore. It was used when reflections were tuned by adjusting for maximum power (corresponding to conjugate match). Now the various mismatch errors have been reduced to the point where the tedious tuning at each frequency is not worth the effort. In fact, modern techniques without tuning might possibly be more accurate because the tuners may introduce their own errors that cannot always be accounted for exactly.

Mismatch in power measurements generally causes the indicated power to be different from that absorbed by a reflectionless power sensor. The reflection from the power sensor is partially accounted for by the Calibration Factor of the sensor which is considered in the next chapter. The interaction of the sensor with the generator (the re-reflected waves) could be corrected only by knowledge of phase and amplitude of both reflection coefficients, Γ_ℓ and Γ_g. If only the standing wave ratios or reflection coefficient magnitudes ρ_g and ρ_ℓ are known, then only the mismatch uncertainty limits can be calculated. The mismatch uncertainty is combined with all the other uncertainty terms in the next chapter where an example for a typical measurement system is analyzed.

$\rho_g = |\Gamma_g|$

$\rho_\ell = |\Gamma_\ell|$

---

* A complimentary HP Reflectometer/Mismatch Error Limits Calculator is available from any Hewlett-Packard sales office, or write to Inquiries Manager at 1507 Page Mill Road, Palo Alto, California 94304.

VI. Errors and Total Uncertainty

Power measurements are so important to developing, specifying, and evaluating rf and microwave systems and components, that it is very important to know the measurement accuracy. The measurement accuracy is quantitatively expressed by uncertainty. Uncertainty is defined as "the assigned allowance for error." The purpose of this chapter is to discuss the errors of power measurement and to show methods of expressing the total uncertainty of measurement.

Power Sensor Errors

The most prevalent errors associated with the power sensor are the mismatch loss and mismatch uncertainty discussed in the previous chapter. A second source of error is the imperfect efficiency of the power sensor.

Effective Efficiency

For most electrical components, efficiency is defined as the ratio of useful output power to total input power. For a power sensor the "power in" is the net power delivered to the sensor; it is the incident power minus the reflected power ($P_i - P_r$). But not all that power is dissipated in the element of the power sensor. Some might be radiated into space or leaked into the instrumentation, some is dissipated in the conducting walls of the power sensor, or in a capacitor, or a number of other places that are not metered by the instrumentation. The metered power indicates only the power which is dissipated in the power sensing element itself.

In order to be metered, the dissipated high frequency power must go through some sort of conversion process to an equivalent dc or low frequency level. The dc or low frequency equivalent is called P_{sub} for substituted power. There are errors associated with the substitution process. In thermistor sensors, for example, errors result from the fact that the spatial distributions of current, power, and resistance within the thermistor are different for dc and rf power.

To accommodate both the usual parasitic losses as well as the dc or low frequency substitution problem mentioned, a special term, effective efficiency η_e, has been adopted for power sensors. Effective efficiency is defined by

$$\eta_e = \frac{P_{sub}}{P_{g\ell}} \qquad (6\text{-}1)$$

$P_{g\ell}$ is the net power absorbed by the sensor during measurement. P_{sub} is the substituted low frequency equivalent for the rf power being measured. For thermistor sensors P_{sub} is the change in bias power required to bring the thermistor back to the same resistance as before the application of rf power. For thermocouple and diode sensors, P_{sub} is the amount of power from a reference power source, at a specified frequency, that yields the same voltage to the metering circuits as $P_{g\ell}$. η_e normally changes with frequency, but changes with power level are usually negligible. Effective efficiency is normally measured by the manufacturer when calibrating the sensor.

Calibration Factor

There is another, more frequently used term that has been defined for power measurements. It combines effective efficiency and mismatch loss and is called the calibration factor K_b. K_b is defined by

$$K_b = \frac{P_{sub}}{P_i} \qquad (6\text{-}2)$$

where P_i is the incident power to the sensor. The accurate measurement of calibration factor K_b is quite involved and performed mainly by standards laboratories and manufacturers. The measurement technique is discussed in other Application Notes of this series.

The definitions of K_b and η_e can be combined to yield

$$K_b = \eta_e \frac{P_{g\ell}}{P_i} = \eta_e (1 - \rho_\ell{}^2) \qquad (6\text{-}3)$$

where ρ_ℓ is the sensor reflection coefficient. The relationship on the right, which is found by substituting for P_i and $P_{g\ell}$ from equations (5-17) and (5-19), shows that K_b is a combination of effective efficiency and mismatch loss.

Most modern power meters have the ability to correct the meter reading by setting a dial to the proper value of K_b. Then P_i is actually read off the meter. Values of K_b for various frequencies are indicated on each Hewlett-Packard power sensor. When this feature is used the indicated or metered power P_m is (using equation 5-17)

$$P_m = \frac{P_{gzo}}{K_b} = P_i = \frac{|b_s|^2}{|1 - \Gamma_\ell \Gamma_g|^2} \qquad (6\text{-}4)$$

But the desired quantity is usually not P_i to the sensor but P_{gzo}, the power that would be dissipated in a Z_o load. Since P_{gzo} is by definition $|b_s|^2$, the ratio of P_{gzo} to the meter indication is

$$\frac{P_{gzo}}{P_m} = |1 - \Gamma_\ell \Gamma_g|^2 \qquad (6\text{-}5)$$

The right side of (6-5) is the mismatch uncertainty. The use of K_b corrects for efficiency and mismatch loss—only the mismatch uncertainty remains. It should be pointed out that there is an additional, unavoidable

uncertainty associated with K_b: that due to inaccuracies in the measurement of K_b by the manufacturer or standards laboratories.

Power Meter Errors

There are a number of errors associated with the electronics inside the power meter. The effect of these errors is to create a difference between P_m and P_{sub}/K_b in equation (6-4).

Reference Oscillator Uncertainty

Open-loop power measurements, such as those that use thermocouples or semiconductor diode sensors, require a known source of power to verify and adjust for the sensitivity of the sensor. Many power meters, such as the HP 435A and 436A, have a stable power reference built in. No matter what power reference is used, if it deviates from the expected power output the calibration adjustment is in error. The uncertainty in the power output from the reference oscillator is specified by the manufacturer. Thermistor power measurements, being closed loop and having no need for a reference oscillator, are free of this error.

Reference Oscillator Mismatch Uncertainty

The reference oscillator has its own reflection coefficient at the operating frequency. This source reflection coefficient, together with that from the power sensor, creates its own mismatch uncertainty. Because the reference oscillator frequency is low, where the reflection coefficients are small, this uncertainty is small (approximately ±0.01 dB or ±0.2%).

Instrumentation Uncertainty

Instrumentation uncertainty is the combination of such factors as meter tracking errors, circuit nonlinearities, range-changing attenuator inaccuracy, and amplifier gain errors. The accumulated uncertainty is guaranteed by the instrument manufacturer to be within a certain limit.

There are other possible sources of uncertainty that are by nature or design so small as to be included within the instrumentation uncertainty. An example of one such error is the thermoelectric voltage that may be introduced by temperature gradients within the electronic circuits and interconnecting cables. Proper design can minimize such effects by avoiding junctions of dissimilar metals at the most sensitive levels. Another example is the small uncertainty which might result from the operator's interpolation of the meter indication.

±1 Count

On meters with digital output, there is an ambiguity in the least significant digit of ± one-half count. On some power meters, such as the HP 436A, this uncertainty is so small that it is absorbed in the instrumentation uncertainty. In some applications, such as relative power measurements or the ratio of two power measurements where most of the causes of instrumentation uncertainty do not affect the final result, this uncertainty is still applicable. In the case of relative power measurements, the uncertainty applies twice, once during the measurement of each power, for a total uncertainty of ± one count. One way of expressing the error is $1/P_{mant}$ where P_{mant} is the mantissa only of the meter indication. Another way is to find the relative power value of the least significant digit (lsd); the uncertainty is $\pm P_{lsd}/P_{ind}$. This uncertainty can be reduced by using an external digital voltmeter of greater resolution.

Zero Set

In any power measurement, the meter must initially be set to "0" with no rf power applied to the sensor. Zero-setting is usually accomplished within the power meter by introducing an offset voltage that forces the meter to read zero. The offset voltage is contaminated by several sources including sensor and circuit noise and setability of the zero set. The zero-set error is specified by the manufacturer, especially for the most sensitive range. On higher power ranges, error in zero-setting is small in comparison to the signal being measured.

Zero Carryover

Most modern power meters, as a matter of convenience, have internal circuitry that eliminates the need to zero-set the power meter every time the power measurement range is changed. If the user zero-sets on the most sensitive range, he is then able to measure power on whatever range is of interest without re-zeroing. The circuitry that allows the zero set to "carryover" to the other ranges may have slight offsets. In principle, zero carryover uncertainty can be eliminated by zero-setting the power meter on the exact range of measurement. This practice is not recommended, however, for the HP 432A, 435A, and 436A Power Meters. The zero carryover for these meters is typically much less than the data-sheet specification and the automatic zero-setting circuits operate more satisfactorily on the most sensitive range.

Noise

Noise is also known as short-term stability and it arises from sources within both the power sensor and circuitry. One cause of noise is the random motion of

free electrons due to the finite temperature of the components. The power observation might be made at a time when this random fluctuation produces a maximum indication, or perhaps a minimum. Noise is specified as the change in meter indication over a short time interval (usually one minute) for a constant input power, constant temperature, and constant line voltage.

Drift

This is also called long-term stability. It is the change in meter indication over a long time (usually one hour) for a constant input power, constant temperature, and constant line voltage. The manufacturer may state a required warm-up interval. In most cases the drift is actually a drift in the zero-setting. This means that for measurements on the upper ranges, drift contributes a very small amount to the total uncertainty. On the more sensitive ranges, drift can be reduced to a negligible level by zero-setting immediately prior to making a reading.

Calculating Total Uncertainty

So far, only the individual errors have been discussed; now a total uncertainty must be found. The case of measuring the power a generator would deliver to a Z_o load, includes almost all the errors discussed. This case is used to demonstrate the calculation of total uncertainty.

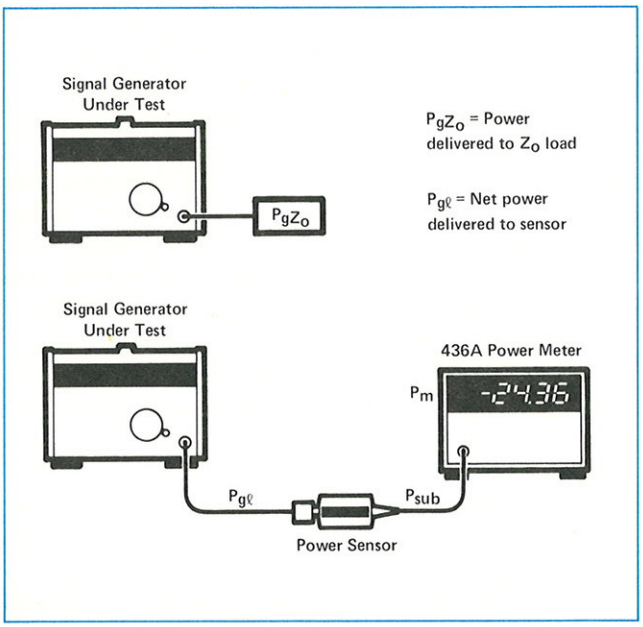

Figure 6-1. Desired power output to be measured is P_{gZo}, but measurement results in the reading P_m.

In some measurement applications, certain sources of error do not enter into the final uncertainty. An example of this is relative power measurement where the ratio of two power measurements is to be found. With proper procedure, the reference oscillator uncertainty affects the numerator and denominator in exactly the same way and therefore cancels out in the final result. In this same application, however, other errors might accumulate — such as the ± half-count error. Such applications are discussed and evaluated in other Application Notes of this series.

Power Measurement Equation

The purpose of this section is to develop an equation that shows how a power meter reading P_m is related to the power a generator would deliver to a Z_o load, P_{gZo} **(Figure 6-1).** The equation will show how the individual uncertainties contribute to the difference between P_m and P_{gZo}.

Starting from the generator in lower part of **Figure 6-1,** the first distinction is that the generator dissipates power $P_{g\ell}$ in the power sensor instead of P_{gZo} because of mismatch effects. That relationship, repeated from Chapter 5, is

$$P_{gZo} = \frac{|1 - \Gamma_\ell \Gamma_g|^2}{1 - |\Gamma_\ell|^2} P_{g\ell} \qquad (6\text{-}6)$$

The next distinction in **Figure 6-1** is that the power sensor converts $P_{g\ell}$ to the dc or low frequency equivalent P_{sub}, for eventual metering. But this conversion is not perfect due to effective efficiency η_e. If $P_{g\ell}$ is replaced by P_{sub}/η_e from equation (6-1), then (6-6) becomes

$$P_{gZo} = |1 - \Gamma_\ell \Gamma_g|^2 \frac{1}{\eta_e (1 - \rho_\ell{}^2)} P_{sub} \qquad (6\text{-}7)$$

The first factor on the right is the mismatch uncertainty term M_u, discussed in the previous chapter. The denominator of the second factor is the Calibration Factor K_b from equation (6-3). Now (6-7) can be written

$$P_{gZo} = M_u \frac{1}{K_b} P_{sub} \qquad (6\text{-}8)$$

The last distinguishing feature of **Figure 6-1** is that the meter indication, P_m, differs from P_{sub}. There are many possible sources of error in the power meter electronics that act like improper amplifier gain to the input signal P_{sub}. These include uncertainty in range-changing attenuators and calibration-factor amplifiers, imperfections in the metering circuit and other sources totaled as instrumentation uncertainty. For open-loop power measurements this also includes those uncertainties associated with the calibration of amplifier gain

with a power-reference oscillator. These errors are included in the symbol m for magnification.

There are other errors associated with the electronics that cause deviation between P_m and P_{sub}. When P_{sub} is zero, then P_m should be zero. Improper zero setting, zero carryover, drift, and noise are likely contributors to P_m not being zero. The meter reading is offset or translated from mP_{sub} by a total amount t. A general linear equation gives P_m in terms of P_{sub}

$$P_m = mP_{sub} + t \qquad (6\text{-}9)$$

Substituting (6-9) into (6-8) gives the power measurement equation

$$P_{gZo} = \frac{M_u (P_m - t)}{K_b m} \qquad (6\text{-}10)$$

In the ideal measurement situation, M_u has the value of one, the $K_b m$ product is one, and t is zero. Under ideal conditions, meter reading P_m gives the proper value of P_{gZo}.

Worst Case Uncertainty

One value of total uncertainty frequently assigned to a power measurement is the worst-case uncertainty. This situation comes about if all the possible sources of error were at their extreme values and in such a direction as to add together constructively and therefore achieve the maximum possible deviation between P_m and P_{gZo}. **Figure 6-2** is a chart of the various error terms for the power measurement of **Figure 6-1.** The measurement conditions listed at the top of **Figure 6-2** are taken as an example. The conditions and uncertainties listed are typical and the calculations are for illustration only. The calculations do not indicate what is possible using the most accurate technique. The description of most of the errors is from a manufacturer's data sheet. Calculations are carried out to four decimal places because of calculation difficulties with several numbers of almost the same size.

Instrumentation uncertainty i is frequently specified in percent of full scale (full scale = P_{fs}). The contribu-

Measurement Conditions: $P_m = 50\ \mu W$; Full Scale (F.S.) $= 100\ \mu W$; $\rho_e \leq 0.091$ ($SWR_e \leq 1.2$); $\rho_g \leq 0.2$ ($SWR_g \leq 1.5$); $K_b = 93\% \pm 3\%$ (worst case), $\pm 1.5\%$ (rss)

Uncertainty Contributions:

Error	Description	Extreme Values		dB		rss Component
		$P_{gZo\ max}$	$P_{gZo\ min}$	+	−	$(\Delta X/X)^2$
M_u	$(1 \pm \rho_g \rho_e)^2$	1.0367	0.9639	0.1565	0.1596	$(0.0367)^2$
K_b Uncertainty	±3% (w.c.), ±1.5% (rss)	0.97	1.03	0.1323	0.1284	$(0.015)^2$
Components of m:						
Ref. Osc. Unc.	±1.2%	0.988	1.012	0.0524	0.0518	$(0.012)^2$
Ref. Osc. M_u	$SWR_g = 1.05$, $SWR_e = 1.1$	0.998	1.002	0.0087	0.0087	$(0.002)^2$
Instrumentation	±0.5% of F.S.	0.99	1.01	0.0436	0.0432	$(0.01)^2$
Total m		0.9762	1.0242	0.1047	0.1037	
Components of t:						
Zero Set	±0.5% F.S. (low range)	−0.05 μW	+0.05 μW			$(0.001)^2$
Zero Carryover	±0.2% of F.S.	−0.2 μW	+0.2 μW			$(0.004)^2$
Noise	±0.025 μW	−0.025 μW	+0.025 μW			$(0.0005)^2$
Total t		−0.275 μW	+0.275 μW	0.0238	0.0239	
Expressions of total uncertainty:						
$P_{gZo\ max}$	equation (6-13)	55.0421 μW				
$P_{gZo\ min}$	equation (6-14)		45.4344 μW			
ΔP_{gZo}		5.0421 μW	−4.5656 μW			
$\Delta P_{gZo}/P_m$		+10.08%	−9.13%			$(0.001837)^{1/2} = \pm 4.3\%$
dB		0.4171 dB	−0.4159 dB	0.4173 dB	−0.4159 dB	+0.1823 −0.1903 dB

Figure 6-2. Chart of uncertainties for a typical absolute power measurement.

tion to magnification uncertainty is

$$m_i = \frac{(1 + i)\, P_{fs}}{P_m} \qquad (6\text{-}11)$$

The several uncertainties that contribute to the total magnification uncertainty m, combine like the gain of amplifiers in cascade. The minimum possible value of m occurs when each of the contributions to m is a minimum. The minimum value of m (=0.9762) is the product of the individual factors (=0.988 * 0.998 * 0.99).

The factors that contribute to the total offset uncertainty t, combine like voltage generators in series; that is, they add. Once t is found, the contribution in dB is calculated from

$$t_{dB} = 10 \log \left(1 \pm \frac{t}{P_m}\right) \qquad (6\text{-}12)$$

The maximum possible value P_{gZo}, using (6-10) and substituting the values of **Figure 6-2,** is

$$P_{gZo\ max} = \frac{M_{u\ max}\,(P_m - t_{min})}{K_{b\ min}\, m_{min}} \qquad (6\text{-}13)$$

$$= \frac{1.0367\ (50\ \mu W + 0.275\ \mu W)}{(0.97)\ (0.9762)}$$

$$= 55.0421\ \mu W = 1.1008\ P_m$$

In (6-13) the deviation of $K_b m$ from the ideal value of one, is used to calculate P_{gZo} max. In the same way the minimum value of P_{gZo} is

$$P_{gZo\ min} = \frac{M_{u\ min}\,(P_m - t_{max})}{K_{b\ max}\, m_{max}} \qquad (6\text{-}14)$$

$$= \frac{0.9639\ (50\ \mu W - 0.275\ \mu W)}{(1.03)\ (1.0242)}$$

$$= 45.4344\ \mu W = 0.9087\ P_m$$

The uncertainty in P_{gZo} may be stated in several other ways:

(1) As an absolute differential in power

$$\Delta P_{gZo} = P_{gZo\ \substack{max \\ min}} - P_m = \begin{matrix} +\ 5.0421 \\ -\ 4.5656 \end{matrix}\ \mu W \qquad (6\text{-}15)$$

(2) As a fractional deviation

$$\frac{\Delta P_{gZo}}{P_m} = \frac{\begin{matrix} +5.0421 \\ -4.5656 \end{matrix}}{50} = \begin{matrix} +0.1008 \\ -0.0913 \end{matrix} \qquad (6\text{-}16)$$

(3) As a percent of the meter reading

$$100 \times \frac{\Delta P_{gZo}}{P_m} = \begin{matrix} +10.08 \\ -9.13 \end{matrix}\ \% \qquad (6\text{-}17)$$

(4) As dB deviation from the meter reading

$$dB = 10 \log \left(\begin{matrix} 1.1008 \\ 0.9087 \end{matrix}\right) = \begin{matrix} +0.4171 \\ -0.4159 \end{matrix}\ dB \qquad (6\text{-}18)$$

An advantage to this last method of expressing uncertainty is that this number can also be found by summing the individual error factors expressed in dB.

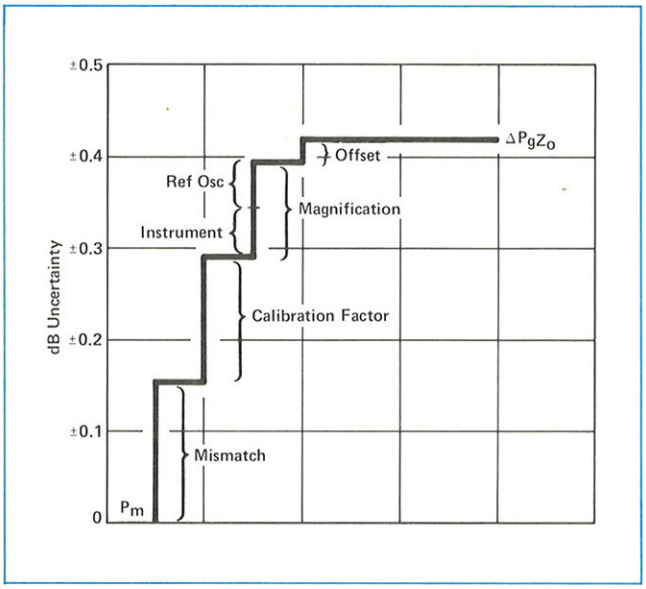

Figure 6-3. Graph of individual contributions to the total worst-case uncertainty.

A graph of contributions to worst-case uncertainty shows that mismatch uncertainty is the largest single component of total uncertainty. This is typical of most power measurements. Magnification and offset uncertainties, the easiest to evaluate from specifications and often the only uncertainties evaluated, contribute less than one-third of the total uncertainty.

RSS Uncertainty

The worst-case uncertainty is a very conservative approach. The probability of the true value of P_{gZo} being near the extreme of such worst-case uncertainty is almost zero. This is because the probability of every error source being at its extreme value and in the worst possible direction is almost zero.

A more realistic method of combining uncertainties, that is gaining in popularity, is the root-sum-of-the-squares (rss) method. The rss uncertainty is based on the fact that most of the errors of power measurement, although systematic and not random, are independent of each other. Since they are independent they are random with respect to each other and combine like random variables. The rss method of combining random variables is justified by statistical considerations that are beyond the scope of this Application Note.

Finding the rss uncertainty requires that each individual uncertainty be expressed in fractional form. The method of calculation follows the name—square the components, sum those squares, then take the square root. The rss uncertainty for the power measurement equation (6-10) is

$$\frac{\Delta P_{gZo}}{P_{gZo}} = \left[\left(\frac{\Delta M_u}{M_u} \right)^2 + \left(\frac{\Delta K_b}{K_b} \right)^2 + \left(\frac{\Delta m}{m} \right)^2 + \left(\frac{\Delta t}{P_m} \right)^2 \right]^{1/2} \quad (6\text{-}19)$$

Each of the factors of (6-19), if not known directly, is also found by taking the rss of its several components. Thus

$$\frac{\Delta m}{m} = \left[\left(\frac{\Delta m_1}{m_1} \right)^2 + \left(\frac{\Delta m_2}{m_2} \right)^2 + \cdots \right]^{1/2} \quad (6\text{-}20)$$

Where m_1, m_2, etc. are the reference oscillator uncertainty, the instrumentation uncertainty, etc. of **Figure 6-2.**

The extreme right hand column of **Figure 6-2** shows the components used to find the total rss uncertainty. The result is ±4.3%, which is much less than the worst-case uncertainty of +10.1%, −9.1%. One characteristic of the rss method is that the final result is always larger than the largest single component of uncertainty.

The many errors of a typical power measurement have been discussed. Although there are several causes of error, some contribute to the indicated reading by amplifying or attenuating the true value. Other causes of error tend to cause offsets in the true value. Total uncertainty is calculated by two popular methods, worst-case uncertainty and root-sum-of-the-square uncertainty. The worst-case uncertainty is pessimistic. The rss uncertainty probably gives a more likely indication of expected performance.

VII. Power Measurement Instrumentation Compared

All the discussion so far about power measurement still leaves the important question: what power meter and sensor should be used for measurement? Each method of measuring average power has some advantages over the others, so the answer to that question becomes dependent on the particular measurement situation. Factors such as cost, frequency range, the range of power levels to be measured, the importance of processing data, accuracy, speed of measurement, and the skill of the personnel involved take on varying degrees of importance in different situations. This chapter compares the measurement systems from several aspects in order to aid in the decision-making process for any application.

Accuracy vs. Power Level

The first comparison of power measuring systems demonstrates the accuracy and power range of each method. **Figure 7-1** shows plots of the maximum worst-case uncertainty when measuring power at various levels. The three parts of this figure are divided according to the type of power meter rather than strictly according to the power sensing method. The reason for dividing the systems this way is that, as far as the user is concerned, there is little need to know whether the sensor works on the diode principle or on the thermocouple principle; he is more interested in the accuracy and power range of measurement. The top graph shows a thermistor sensor and its bridge type power meter. The second graph shows the range of sensors that work with the analog HP 435A Power Meter. The sensors are of two types—the low-barrier Schottky diode (LBSD) sensor and two different thermocouple sensors. The third graph shows a digital instrument, the HP 436A Power Meter, using the same sensors as for the HP 435A.

Figure 7-1 shows that the LBSD and thermocouple power sensors together cover a 105 dB range of power levels with only three sensors. The 8481H Power Sensor, which covers the high power end of that range, contains the same thermocouple sensor as the 8481A, except it is preceded by a 20 dB attenuator. Using an attenuator this way translates the measurement range of the sensor upward. For the 8481H, the attenuator is integrated with the thermocouple so the reflection coefficient and calibration factor specified by the manufacturer apply to the combination. The broad power range covered by interchangeable sensors is a considerable advantage over the thermistor based measurement systems.

A comparison of the top two graphs of **Figure 7-1,** shows that the accuracy of the thermistor based systems is substantially the same as for the thermocouple based system with an analog meter for output. The thermocouple sensor has the best reflection coefficient but the thermistor system does not require a power-reference oscillator and its additional uncertainty. These two effects tend to offset each other for this application. The accuracy difference between the two systems is too small to effectively say that one system is better on that basis. The significant advantage of the 435A based measurement is the flexibility of being able to use other sensors and, once having the sensors, of being able to change to the digital 436A Power Meter if needed.

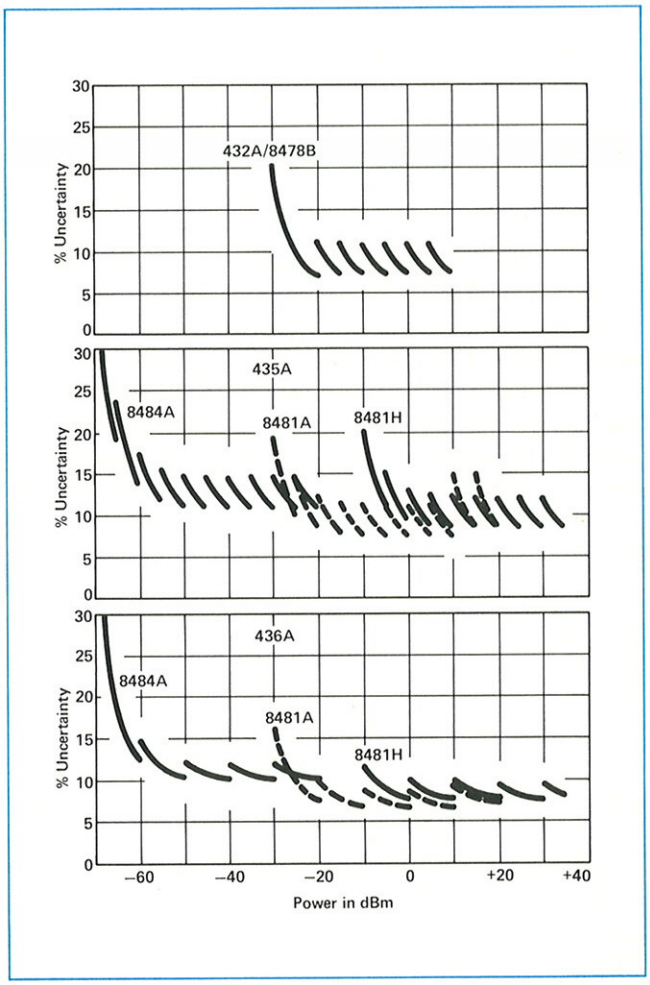

Figure 7-1. Worst-case uncertainty vs. power from data sheet specs for $\rho_s = 0.091$ (SWR = 1.2) and f = 2 GHz: (top) analog thermistor mount system; (middle) analog power meter system using LBSD sensors and thermocouple sensors; (bottom) digital power meter using LBSD and thermocouple sensors.

The third graph of **Figure 7-1,** for the 436A Power Meter, when compared to the graph for the 435A, shows one of the advantages possible with a digital system. Analog meters, such as in the 435A, are limited by mechanical problems in the meter that cause instrumentation uncertainty to be stated in percent of full scale. At the low end of each range the uncertainty becomes fairly large when expressed as a percent of the reading. Digital systems are free of these problems and, with proper design, have better accuracy. The instrumentation accuracy for a digital meter can be specified as a percent of the reading instead of as a percent of full scale. This means that at each range change, there is not such a big change in accuracy for the digital meter. For this reason, the digital power meter does not need so many ranges; each range can cover 10 dB with little change in accuracy across the range. The 436A digital power meter is more accurate than the 435A analog power meter.

There are a number of reasons for being careful about putting too much value in the accuracy calculations of **Figure 7-1.** First of all, the worst-case uncertainty is calculated from specification limits. Specification limits are strongly dependent on the manufacturers' need to have a good production yield of instruments for the whole family of specifications. A particular measurement system is likely to be very close to one spec limit but meet another spec easily; a second system might reverse the roles. If the root-sum-of-the-squares uncertainty were plotted, taking advantage of the random relationship between specifications, the uncertainties would be much smaller and even closer together. A second reason for caution is that the calculations are done for one particular frequency (2 GHz) and one particular source reflection coefficient (0.091). A different frequency and different source match would give a different overall uncertainty. Sources frequently have a much larger reflection coefficient which would raise the overall uncertainty due to mismatch effects.

Frequency Range and Reflection Coefficient

All three types of HP power sensors have models that cover a frequency range from 10 MHz to 18 GHz with coaxial transmission line. A special version of the thermistor mount goes down to 1 MHz and the HP 8482A and 8482H thermocouple power sensors go down to 100 kHz. The efficiency at each frequency is correctable with the Calibration Factor dial of the power meter, so that it is not particularly critical in deciding on a measurement system.

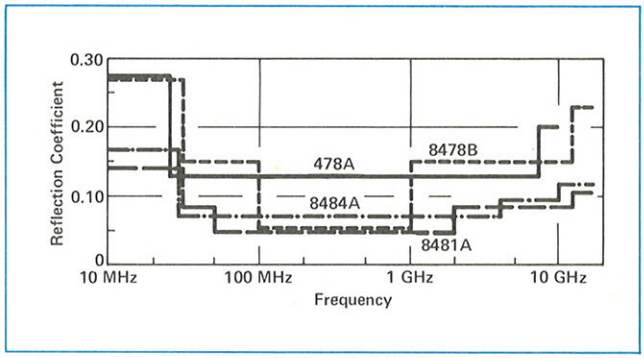

Figure 7-2. Specified reflection-coefficient limits for the HP 478A and 8478B Thermistor Mounts, 8481A Thermocouple Power Sensor, and the 8484A LBSD Power Sensor.

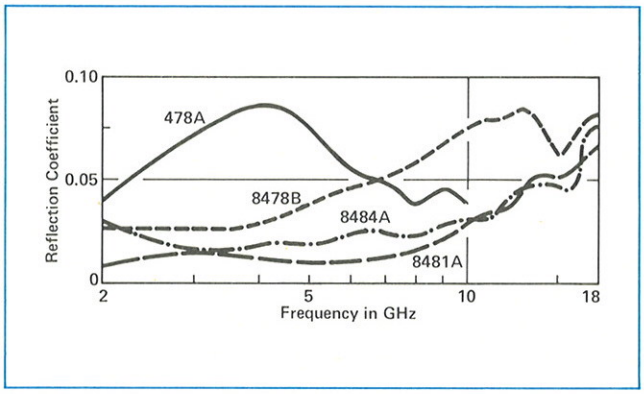

Figure 7-3. The average reflection coefficient from a group of 98 8478B and 108 478A Thermistor Mounts, 127 8481A Thermocouple Sensors, and 15 8484A LBSD Sensors.

The reflection coefficient, however, is very important because it contributes strongly to the mismatch uncertainty, usually the largest source of error. **Figure 7-2** shows the specification limits for the reflection coefficient of two different thermistor mounts, a thermocouple power sensor, and a low-barrier Schottky diode power sensor. **Figure 7-3** shows the average reflection coefficient for a group of each type of power sensor. These graphs indicate that the thermocouple and diode sensors have a lower reflection coefficient than the thermistor sensors.

For power measurements in rectangular waveguide, thermistor mounts have an advantage. Thermistor power measurements are closed loop so there is no need for a low-frequency power reference oscillator. It is an advantage for thermocouple and diode sensors to have a reference oscillator to adjust for sensitivity variations from one sensor to another. Such a low-frequency signal cannot propagate into the sensor through a waveguide input. For waveguide frequencies that overlap the standard coaxial frequencies, thermocouple and diode sensors can be adjusted for calibration using coax, but

then they must have a waveguide-to-coax adapter added. The loss of this adapter and its reflection coefficient obscures the sensor calibration factor, increases the overall reflection coefficient, and increases the uncertainty. Waveguide thermistor mounts need no extra waveguide-to-coax adapter and no calibration adjustment with a reference signal. Thermistor mounts are especially valuable in the millimeter waveguide ranges where waveguide-to-coax adapters are not available.

Speed of Response

To measure weak signals with great accuracy, power meters are designed to have a narrow bandwidth compared to most other electronic circuits. Narrow band circuits are necessary to pass the desired signal but reject the noise that would obscure a weak signal. Narrow bandwidth leads to the long response time. For heat responding power sensors, like the thermistor and thermocouple, response time is also limited by the heating and cooling time constants of the heat sensing element. The typical thermistor power measurement has a 35 millisecond time constant and 0 to 99 percent response time of about five time constants or 0.175 seconds. The power meters for thermocouple and LBSD sensors have 0 to 99 percent response times of 0.1 to 10 seconds, depending on the range of the power meter. The more sensitive ranges require the longest times.

For manual measurements, the speed of response is seldom a problem. By the time the observer turns on the rf power and is ready to take data, the power meter has almost always reached a steady reading.

For analog systems applications, where the power meter output is being used to control other instruments, the power meter acts like a low pass filter. The equivalent cutoff frequency of the filter has a period roughly the same as the 0 to 99 percent response time. For signals where the power changes too rapidly for the power meter to respond, the power meter averages the power. When a power meter is being used to level the output of a signal generator whose frequency is being swept, the speed of the frequency sweep may have to be reduced to allow the power meter time to respond to the power level changes.

There is no clear-cut advantage with regard to speed of one power measurement system over another. In some power ranges one system is faster, and in other ranges another system is faster. If response time is important, manufacturers' data sheets should be compared for the particular application.

Susceptibility to Overload

The maximum rf power that may be applied to a power sensor is limited in three ways. The first limit is an average power rating. Too much average power usually causes damage because of excessive heat. The second limit is the energy in a pulse. If the pulse power is too high for a short time, in spite of the average power being low, the pulses cause a temporary hot spot somewhere in the sensor. Damage occurs before the heat has time to disperse to the rest of the sensor. The third limit is peak envelope power. This limit is usually determined by breakdown phenomena that damage sensor components. The limits are usually stated on the manufacturer's data sheet. None of the three limits should be exceeded. The power limits of any sensor may be moved upward by adding an attenuator to absorb the bulk of the power. Then the power limits are likely to be dictated by the attenuator characteristics.

	8478B Thermistor Mount	8484A LBSD Sensor	8481A Thermocouple Sensor	8481H Thermocouple Sensor
Max Average Power	30 mW	200 mW	300 mW	3.5 W
Max Energy Per Pulse	10 W·μs		30 W·μs	100 W·μs
Peak Envelope Power	200 W	200 mW	15 W	100 W

Figure 7-4. Maximum power limits of various power sensors.

A chart of power limits **(Figure 7-4)** shows that the HP 8481H Power Sensor, which consists of an attenuator followed by a thermocouple sensor, excels in all respects, except for peak envelope power where the thermistor mount is better. One characteristic, that might be important but not obvious from the chart, is the ratio of maximum average power to the largest measureable power. The LBSD sensor can take 200 mW (+23 dBm) of average power, while the high end of its measurement range is 10 μW (−20 dBm). This means that the LBSD is forgiving in situations where the power level is accidentally set too high. A mistake of 10 dB in setting an output attenuator while measuring power, will merely read off scale for the HP 8484A. The same mistake might damage the other sensors. Excessive power is, by far, the primary cause of power sensor failure.

Automated Power Measurement

Digital power meters that are programmed for automatic operation, like other automated systems, have advantages over manual measurements. They can gather data rapidly, the data can be processed, and the system can be operated by relatively unskilled personnel. Even in a manual mode, digital indications are less prone to the human error of misinterpreting the meter scale and using wrong range multipliers. In the case of power measurement, there are additional advantages to automatic systems. Successive measurements can be tested to assure that the power measurement has reached steady state and several successive readings can be averaged to reduce the effects of noise.

Although digital output of the power level would be quite an advantage by itself, complete digital control of range selection, zero-setting, and triggering the power meter at a particular time is required by most automatic measurement systems. The HP 436A Power Meter can be purchased with full remote-control capability while still maintaining its manual capabilities. This automatic capability, or the ability to expand into automatic systems at a future date, could be the deciding factor in using the 436A Power Meter with its thermocouple and LBSD sensors.

In most situations the decision about which measurement system to use will probably come to be one of flexibility compared to cost. The flexibility comes in the form of the possibility for automatic measurement and of a large range of measurement. Accuracy and speed of response are substantially the same in the systems discussed, with the advantage going to a digital power meter. Specifications are likely to change with time, as is cost, so current data sheets should be consulted.

VIII. Instruments for Peak Power Measurements

Measurement of pulse power has been a frequent requirement in microwave work since the early development of pulse radar. Various approaches to pulse power measurement include the following techniques: (1) Average Power-Duty Cycle; (2) Notch Wattmeter; (3) Direct Pulse; (4) DC-Pulse Power Comparison; (5) Barretter Integration-Differentiation; and (6) Sample and Hold.

The first three methods involve the interconnection and use of a number of standard instruments such as crystal detectors, bolometers, and oscilloscopes. These three methods seem to fall into the category of techniques rather than of instrumentation principles. They will therefore be discussed in another part of this Application Note series. The remaining three methods, however, do include special equipment so they are discussed here.

DC-Pulse Power Comparison

An example of the DC—Pulse Power Comparison technique is the use of the HP 8900B Peak Power Calibrator. Unlike some systems, the 8900B does not rely on pulse width or on repetition rate measurements for its accuracy. The 8900B Peak Power Calibrator provides the opportunity to measure either pulse power or peak envelope power.

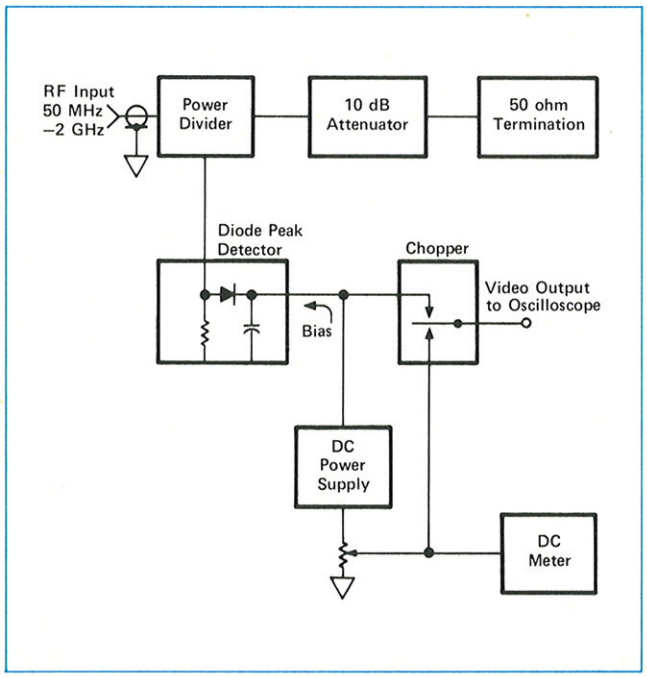

Figure 8-1. Block diagram of HP 8900B Peak Power Calibrator.

The block diagram of the HP 8900B, **(Figure 8-1),** shows that a power divider splits the input pulse and feeds part of it to a diode peak detector. The peak detector develops a dc level proportional to the peak voltage of the input rf pulse. The diode is forward-biased to bring its operating point to a satisfactory impedance level for following pulse envelopes. The voltage developed by the diode is connected to one contact of a mechanical chopper. A regulated dc supply provides a variable comparison voltage which is fed to the other contact of the chopper and also to a dc meter calibrated in terms of power. The center arm of the chopper alternately switches between the detector output and the dc supply. This allows an oscilloscope comparison of the two outputs at the video output jack. The static dc bias on the diode is effectively erased from the video output by a front panel null control. This control, adjusted like the zero-set of average power meters, permits compensation for long-term diode changes.

In operation, unknown pulsed power is applied to the 8900B input, the envelope is detected and displayed on an oscilloscope. The dc voltage supplied by the 8900B is adjusted for coincidence with the detected peak pulse amplitude. At this point the dc voltage is equal to the peak pulse voltage input, and the meter indicates the equivalent peak envelope power.

Although some of the power is directed to the peak detector, the remainder of the power is fed to a 10 dB attenuator and 50 ohm termination. This power is convenient for calibrating the instrument. If the 50 ohm termination is replaced by an accurate average power measurement system and a CW power source is applied to the 8900B input connector, the effect of applied power can be monitored on the average-reading CW power standard and the peak-reading diode detector simultaneously. Only the attenuation between the input connector and the CW standard needs to be known to determine the effect of a known power level on the peak detector. The 10 dB pad reduces the input power so average-reading power meters may be used for calibration.

The HP 8900B enables convenient and rapid power measurements of pulses greater than 0.25 μs in duration at rf frequencies of 50 MHz to 2 GHz. Pulse repetition rates (PRF's) up to 1.5 MHz may be measured because of the wideband detector. The 0.25 μs specification gives the peak detector time to charge to the true peak value of an input pulse; 0.1 μs is a more realistic limit with normal cable lengths and oscilloscopes connected

to the video output. Overall accuracy is ±1.5 dB, but an optional correction chart for frequency effects reduces this error to ±0.6 dB maximum. This accuracy is based on an absolute worst-case error analysis which includes the following sources of error: (1) attenuation measurement between the input connector and 10 dB pad output; (2) the average power measurement; (3) mismatch; (4) meter tracking and repeatability; (5) aging effects on detector diode; and (6) readout resolution.

Barretter Integration-Differentiation

Peak power meters are available which operate in conjunction with barretter mounts and special barretter elements that integrate the pulsed power input. The integration comes from the barretter's comparatively long thermal time constant (greater than 120 μs). The barretter forms one leg of a Wheatstone bridge that receives excitation and bias current from a constant current supply. Input pulses to the barretter change the element resistance resulting in a bridge output signal which is the integral of the pulses. By amplifying and differentiating the bridge signal, the input pulse shape is reconstructed. The reconstructed pulses are peak detected in a voltmeter circuit calibrated in peak power. Pulse sensitivity characteristics of the barretter must be known in order to translate the relative pulse amplitude to an absolute power level. Calibration of typical peak power meters using the Barretter Integration technique is based on: (1) previous measurements of representative barretter output-per-milliwatt input-per-microsecond (pulse sensitivity) and (2) a calibrating signal generator used in adjusting amplifier gain so that a predetermined level is indicated on the meter before measuring pulse power.

While the characteristics of the amplifier and differentiator are important considerations, the barretter's thermal time constant is the basic limitation to pulse width and repetition rate as well as maximum input power capability. If the pulse is too narrow, the barretter cannot heat enough to provide a signal above the noise level of the amplifier. As the pulse width approaches the barretter thermal time constant, the integration by the barretter becomes less accurate. Maximum input power to the barretter is, of course, limited by the physical characteristics of the element, which has the usual barretter susceptibility to damage by overload.

Typically the pulse width is specified at 0.25 μs minimum to 10 μs maximum with a PRF of 50 to 10000 pulses per second. Pulses up to about 300 mW peak may be handled within the duty cycle specified for the system.

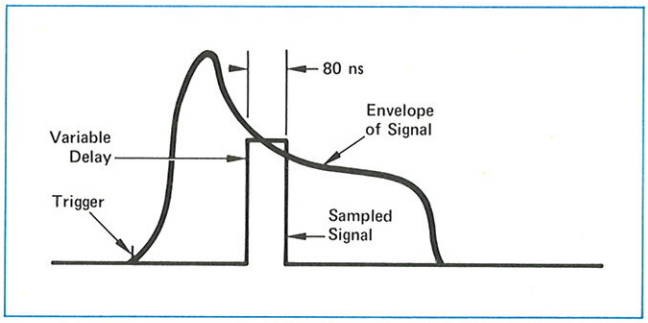

Figure 8-2. The envelope of a microwave pulse modulated signal and the sampled signal. The value of the signal during the sampling time is displayed to indicate power.

Sample and Hold

The sample and hold method of making pulse power measurements relies on the ability of a diode detector to follow the envelope of a pulsed microwave signal **(Figure 8-2)**. A small portion of that envelope (typically 80 ns) is sampled, stored on a capacitor ("held"), and then amplified and metered. By changing the time delay, the portion of the envelope that is sampled and metered can be adjusted to the pulse maximum. The meter then reads the peak envelope power.

By plotting the power as the delay is precisely varied, a profile of the pulse shape may be constructed. Then the pulse power, as defined in Chapter I, could be calculated.

The small percentage of the total time that the signal is being sampled results in an effectively large noise level and therefore a large minimum detectable signal. The CW diode detectors, with the techniques discussed in previous chapters, could measure levels from −70 dBm to −20 dBm, but this sampling technique covers from −20 dBm to +10 dBm. At these levels the diode detector is not very square-law. But the amplifiers include shaping (gain designed to depend on signal level) to make the diode appear square-law and indicate the output power. Such square-law correction of diode output must be made before the averaging is done; that is, the correcting circuits must be quick enough to follow the modulation waveform. With this sample and hold technique, however, once the signal is "held" it is basically a CW signal and proper correction for diode square-law variation is possible. Still other shaping circuits can be used so the indicated value is in dBm or relative dB.

Measurements using this technique are not limited to pulsed signals. Sampling a CW signal is not only valid, but it is a convenient means of calibrating the meter. Pulses as narrow as 0.35 μs may be measured without correction and pulses as narrow as 0.2 μs may be measured with correction.

References

Beatty, R. W. "Intrinsic Attenuation," *IEEE Trans. on Microwave Theory and Techniques,* Vol. 11, No. 3 (May, 1963) 179-182.

Beatty, R. W. "Insertion Loss Concepts," *Proc. of the IEEE,* Vol. 52, No. 6 (June, 1966) 663-671.

Carmean, D. "More Conveniences in the HP Microwave Power Meter," *Hewlett-Packard Journal,* Vol. 6, No. 7 (Mar., 1955).

Edwards, A. P. "Digital Power Meter Offers Improved Accuracy, Hands-Off Operation, Systems Capability" *Hewlett-Packard Journal,* Vol. 27 No. 2 (Oct. 1975) 2-7.

Engen, G. F. "A Refined X-Band Microwave Microcalorimeter," *NBS J. of Res.,* 63C 77 (1959).

Gallagher, W. and Hand, B. P. "New Conveniences for Microwave Power Measurements," *Hewlett-Packard Journal,* Vol. 5, No. 11 (July, 1954).

Ginzton, E. L. *Microwave Measurements.* McGraw-Hill, Inc., 1957.

Hand, B. P. "Direct Reading UHF Power Measurement," *Hewlett-Packard Journal,* Vol. 1, No. 59 (May, 1950).

Hand, B. P. "An Automatic DC to X-Band Power Meter for the Medium Power Range," *Hewlett-Packard Journal,* Vol. 9, No. 12 (Aug., 1958).

Hand, B. P. and Schrock, N. B. "Power Measurement from 10 to 12,400 Megacycles," *Hewlett-Packard Journal,* Vol. 2, No. 7-8 (Mar.-Apr., 1951).

Henning, R. E. "Peak Power Measurement Technique," *Sperry Engineering Review,* (May-June 1955) 10-15.

IEEE Standard Application Guide for Bolometric Power Meters. IEEE Std. 470-1972.

IEEE Standard for Electrothermic Power Meters. IEEE Std. 544-1976.

Jackson, W. H. "A Thin-Film Semiconductor Thermocouple for Microwave Power Measurements," *Hewlett-Packard Journal,* Vol. 26, No. 1 (Sept., 1974) 16-18.

Kuhn, N. J. "Simplified Signal Flow Graph Analysis," *Microwave Journal,* Vol. 6, No. 10 (Nov., 1963) 59-66.

Kurakawa, K. "Power Waves and the Scattering Matrix," *IEEE Trans. on Microwave Theory and Techniques,* Vol. 13, No. 2 (March, 1965) 194-202.

Lamy, J. C. "Microelectronics Enhance Thermocouple Power Measurements," *Hewlett-Packard Journal,* Vol. 26, No. 1 (Sept., 1974) 19-24.

Mason and Zimmerman. *Electronic Circuits, Signals and Systems.* John Wiley and Sons, Inc., 1960.

Montgomery, C. G. *Technique of Microwave Measurements.* Massachusetts Institute of Technology, Radiation Laboratory Series, Vol. 11, McGraw-Hill, Inc., 1948.

"Power Meter—New Designs Add Accuracy and Convenience," *Microwaves,* Vol. 13, No. 11 (Nov., 1974).

Pramann, R. F. "A Microwave Power Meter with a Hundredfold Reduction in Thermal Drift," *Hewlett-Packard Journal,* Vol. 12, No. 10 (June, 1961).

Pratt, R. E. "Very-Low-Level Microwave Power Measurements," *Hewlett-Packard Journal,* Vol. 27, No. 2 (Oct., 1975) 8-10.

Skolnik, M. *Introduction to Radar Systems.* McGraw-Hill, Inc., 1962.

Szente, P. A., Adam, S., and Riley, R. B. "Low-Barrier Schottky-Diode Detectors," *Microwave Journal,* Vol. 19, No. 2 (Feb., 1976).